UNIVERSIDADE FEDERAL DE SANTA MARIA
CENTRO DE CIÊNCIAS RURAIS
PROGRAMA DE PÓS-GRADUAÇÃO EM CIÊNCIA DO SOLO

Alice Prates Bisso Dambroz

FRAGILIDADE AMBIENTAL DA BACIA DO ARROIO GUARDA MOR

Santa Maria, RS
2020

Alice Prates Bisso Dambroz

FRAGILIDADE AMBIENTAL DA BACIA DO ARROIO GUARDA MOR

Dissertação apresentada ao Curso de Pós-Graduação em Ciência do Solo, área de concentração Biodinâmica e Manejo do Solo, da Universidade de Santa Maria (UFSM, RS), como requisito parcial para obtenção do título de **Mestre em Ciência do Solo**.

Orientador: Prof. Dr. Jean Paolo Gomes Minella

Santa Maria, RS
2020

Dambroz, Alice Prates Bisso
Fragilidade ambiental da bacia do Arroio Guarda Mor / Alice Prates Bisso Dambroz.- 2020.
93 p.; 30 cm

Orientador: Jean Paolo Gomes Minella
Dissertação (mestrado) - Universidade Federal de Santa Maria, Centro de Ciências Rurais, Programa de Pós Graduação em Ciência do Solo, RS, 2020

1. Suscetibilidade à erosão 2. Índices topográficos 3. SIG 4. Modelo WATERSED 5. Fingerprinting I. Gomes Minella, Jean Paolo II. Título.

Sistema de geração automática de ficha catalográfica da UFSM. Dados fornecidos pelo autor(a). Sob supervisão da Direção da Divisão de Processos Técnicos da Biblioteca Central. Bibliotecária responsável Paula Schoenfeldt Patta CRB 10/1728.

Alice Prates Bisso Dambroz

FRAGILIDADE AMBIENTAL DA BACIA DO ARROIO GUARDA MOR

Dissertação apresentada ao Curso de Pós-Graduação em Ciência do Solo, da Universidade de Santa Maria (UFSM, RS), como requisito parcial para obtenção do título de **Mestre em Ciência do Solo**.

Aprovada em 23 de julho de 2020:

_____

Jean Paolo Gomes Minella, Dr. (UFSM)
(Presidente/Orientador)

_____

Fabrício de Araújo Pedron, Dr. (UFSM)

_____

Tales Tiecher, Dr. (UFRGS)

Santa Maria, RS
2020

AGRADECIMENTOS

Ao professor Jean Minella pela orientação, confiança e exemplo.

À UFSM e ao PPGCS pelo ensino, estrutura e apoio fornecidos.

À CAPES pelo apoio financeiro.

Ao LANAGRO e à Caroline Tomaszewski, por conceder o espaço, o equipamento e o apoio necessários às análises espectroscópicas. Também agradeço aos professores Tales Tiecher e Cláudia Barros por toda a ajuda durante esse período.

Ao pesquisador Jean Bueno pelo conhecimento compartilhado e auxílio com as análises estatísticas.

Aos professores Fabricio Pedron, Ricardo Dalmolin e ao Grupo de Pedologia da UFSM que construíram o detalhado mapa de solos da bacia do Guarda Mor.

Aos moradores desta bacia que, gentilmente, permitiram a coleta de amostras em suas propriedades.

Aos colegas, em especial aos que compõem o GIPEHS e que tanto me ajudaram, pelos bons momentos, amizade e aprendizado.

Aos meus pais e irmão pelo suporte nas minhas escolhas, pelo incentivo e grande exemplo. A vocês, também dedico este trabalho.

RESUMO

FRAGILIDADE AMBIENTAL DA BACIA DO ARROIO GUARDA MOR

Autor: Alice Prates Bisso Dambroz
Orientador: Prof. Dr. Jean Paolo Gomes Minella

Locais de erosão atuam como fontes de sedimentos e são responsáveis pela transferência de sedimentos, nutrientes e poluentes, levando à degradação dos solos e da água. O processo erosivo ocorre em várias e contínuas escalas. Essa variabilidade não é abrangida por uma única abordagem ou modelo holístico. Ferramentas complementares que integram geomorfologia, modelagem da erosão e produção de sedimentos foram utilizadas para identificar esses locais e compreender suas fragilidades. O estudo foi realizado em três sub bacias hidrográficas, pareadas e ambientalmente frágeis (S1, S2 e S3), embutidas na bacia do arroio Guarda Mor, localizada em uma transição geomorfológica entre o Planalto e a Depressão Central do Rio Grande do Sul. Três pacotes de trabalho (WP) foram analisados. O WP1 aborda zonas de erosão influenciadas pelo terreno, por atributos topográficos primários e secundários. O WP2 consiste em uma simulação dinâmica do escoamento, da erosão e da produção de sedimentos com o modelo WATERSED, agregando ao fator topografia, o clima, o solo e o uso da terra. Por fim, o WP3 identifica fontes de sedimentos por meio de uma técnica alternativa de *fingerprinting*. Os modelos de predição, *support vector machines*, foram construídos com base no espectro de infravermelho próximo das amostras de solo e sedimentos. A declividade, o Índice Topográfico de Umidade, o Índice de Potência do Fluxo e o Fator Topográfico de comprimento de rampa e declividade (Fator LS) mostram um arranjo geomorfológico semelhante para S1 e S3, indicando sua suscetibilidade à erosão ligeiramente maior que a S2. Os locais mais propensos à erosão parecem estar localizados perto da rede de drenagem e das áreas mais íngremes. O mesmo foi indicado pelo WP2, com evidências realçadas por eventos de precipitação de maior magnitude. A sub bacia S2 apresenta maior potencial de escoamento e produção de sedimentos. Os resultados de *fingerprinting* mostram maior contribuição de estradas não pavimentadas para S1 e S2 e de fontes superficiais de solo para S3. Quanto à traçagem de sedimentos dos tributários, os resultados indicam que cerca de 90% dos sedimentos no exutório da bacia do Guarda Mor são originados na S1. O resultado pode ser devido a fontes não amostradas entre fonte e dreno. A combinação das análises forneceu resultados diferentes e complementares. WP1 e WP2 mostram as áreas adjacentes à rede de drenagem para todas as sub bacias como as mais frágeis. Distâncias curtas da fonte ao rio promovem boa conectividade para transferência de material. As semelhanças entre S1 e S3 não resultaram em contribuições de sedimentos semelhantes. O *fingerprinting* agregou informações em relação a importância das estradas não pavimentadas e da erosão na rede de drenagem para a erosão e produção de sedimentos. Esse componente da paisagem não é contemplado pelos WP1 e WP2. Material proveniente do canal fluvial e de fontes superficiais de solo também são fontes significativas de sedimentos. A geomorfologia é capaz de representar a susceptibilidade à erosão destas áreas, mapas mais detalhados podem superar a não representação das estradas. Análises posteriores devem considerar fontes não amostradas entre o exutório das sub bacias e GMex.

Palavras-Chave: Suscetibilidade à erosão. Índices topográficos. SIG. Modelo WATERSED. *Fingerprinting*. Erosão. Modelagem.

ABSTRACT

GUARDA MOR CATCHMENT'S ENVIRONMENTAL FRAGILITY

Author: Alice Prates Bisso Dambroz
Advisor: Prof. Dr. Jean Paolo Gomes Minella

Erosion hotspots act as sediment sources and are responsible for the transfer of sediments, nutrients and pollutants, leading to soil and water degradation. The erosive process occurs on variable and continuous range of scales and this variability is not addressed by a holistic approach or model. Complementary tools that integrate geomorphology, erosion modelling and sediment yield were used to identify such spots and to comprehend their fragilities. The study was carried on three environmentally fragile paired headwater sub catchments (S1, S2 and S3) nested in Guarda Mor catchment, located in a geomorphological transition between the Plateau and Central Depression of Rio Grande do Sul. Three work packs were analyzed. WP1 addresses zones of relief-influenced erosion, by primary and secondary topographic attributes. WP2 consists of a dynamic simulation of runoff, erosion and sediment yield with WATERSED model, adding to topography, climate, soil and land use factors. Last, WP3 identifies sediment sources by means of an alternative fingerprinting technique. Support vector machine prediction models were built based on soil and sediment samples' near-infrared spectrum. Slope, Topographic Wetness Index, Stream Power Index and Slope Length and Steepness Factor (LS Factor) show a similar geomorphological arrangement for S1 and S3, indicating their slightly greater erosive susceptibility than S2. The hotspots seem to be located near the drainage network and steepest areas. The same was indicated by WP2, with increased evidence by higher magnitude rainfall events. The sub catchment S2 shows greater potential for runoff and sediment yield. Fingerprinting results greatest contribution from unpaved roads to S1 and S2 and from topsoil to S3. As for tracing tributaries, results indicate that nearly 90% of sediment at Guarda Mor's outlet come from S1. The result may be due to unsampled sources in between source and sink. The combination of analyses provided different and complementary results. WP1 and WP2 show the areas adjacent to the drainage network for all sub catchments as the most fragile. Short distances from source to river promote good connectivity for material transfer. Similarities between S1 and S3 did not lead to similar sediment contributions. Fingerprinting added information regarding the importance of unpaved roads and erosion in the drainage network to erosion and sediment yield. This landscape component is not addressed by WP1 and WP2. Topsoil and stream channels are also significant sediment sources. Geomorphology can represent these areas' susceptibility to erosion, more detailed maps may overcome the lack of representation of roads. Further analysis should consider unsampled sources between the sub catchments' outlets and GMex.

Keywords: Erosion susceptibility. Topographic indexes. GIS. WATERSED model. Sediment fingerprinting. Erosion. Modeling.

LISTA DE ILUSTRAÇÕES

LISTA DE TABELAS

SUMMARY

1 INTRODUCTION

The erosive process has been accelerated by human activities, especially through inadequate soil management and occupation. Water erosion, through its erosive agents, enhances the loss of the soil's superficial layer, causing losses in its fertility and productivity (JULIEN, 1995), and in agriculture's sustainability, activity that depends on the landscape as much as affects it. The nature of this process is temporally and spatially dynamic, according to factors of the hydrological cycle, soil, geology, vegetation/land use, relief and slope (MORGAN, 2005), which can be observed jointly on a catchment scale.

On the landscape, the number of potential erosion sources is not restricted only to cropfields, as it can also occur on grasslands, forests, unpaved roads and fluvial channels. Just as its effects happen beyond its source site, the eroded sediment causes environmental damages such as pollution, increased floods and decreased water quality (ROBERTSON et al., 2007). Since this process leads to soil and water resources degradation, understanding and spatially identifying hotspots on the landscape can be a means of proposing more suitable soil management and land uses.

Over these landscape components, there are different dominant erosion processes. Raindrop impact and interrill erosion are dominant erosion processes at the top of slopes. At a critical distance from the top, water can accumulate in runoff. Erosion by concentrated and higher runoff rates can be dominant on middle slopes and deposition usually occurs on the lower segments (MORGAN, 2005).

Landscape segments prone to soil loss are considered erosion hotspots, naturally favored source areas of sediments such as steep slopes, shallow and erodible soils. These hotspots act as sediment sources and are responsible for the transfer of nutrients and pollutants, degrading both terrestrial and aquatic environments (GOLOSOV; WALLING, 2019). They can also contribute with large amounts of water from surface runoff to the drainage network. Furthermore, as runoff is generated, accumulated and gains energy, it may result in problems from fluvial processes such as excavation, transport and sedimentation.

In order to obtain greater understanding on the origin of a stream's degradation, the behavior of hydrological and erosive processes occurring within the entire catchment must be analyzed. These processes comprehend a series of phenomena occurring on

variable and continuous range of scales and not assured to be incorporated in a holistic approach or model (GENTINE et al., 2012). The analysis regarding this complexity should, then, combine monitoring and modelling techniques that are able to produce complementary information (MINELLA; MERTEN, 2011).

Along with climate, soil characteristics and land use, topography is one of the basic factors controlling soil erosion. In environments where topography exerts greater effect on water movement, digital elevation model (DEM) analysis is a way of parametrizing phenomena related to an environment's hydrology (GRUBER; PECKHAM, 2009). The acquisition of topographic indexes is useful in identifying spots with higher susceptibility to erosive processes. Topographic indexes characterize both simple and complex terrain attributes and are used to quantify topography's control over physical processes. This was made easier to accomplish with the development of Geographic Information Systems (GIS), by easily performing calculations (GRUBER; PECKHAM, 2009). Buitrago and Martínez (2016), for instance, used DEMs as a data source for calculating topographic attributes and indexes in order to assess the risk of erosion and to better understand the factors affecting erosion. This attributes and indexes have also been used in modelling of hydrological and geomorphological processes (MINELLA; MERTEN, 2012).

Physically based distributed models can be used as a tool for dynamic evaluating the spatial variability of erosion within a catchment and erosion models have been used for identifying erosion hotspots. The physically based Water Erosion Prediction Project (WEPP) model (FLANAGAN; NEARING, 1995) has been used to identify runoff and soil loss risk areas in Colombia (BAIGORRIA; ROMERO, 2007). While the Soil and Water Assessment Tool (SWAT) model was applied to spatially identify erosion hotspots at a sub basin level in Ethiopia (LEMMA et al., 2019).

Besides, the much needed information on sediment provenance can be obtained by the sediment fingerprinting technique (WALLING 2013), which estimates the contribution of different potential sediment sources reaching the fluvial channel. Sediment fingerprinting has been coupled to suspended sediment monitoring to improve knowledge on its sources and to better understand erosion processes within a catchment (EVRARD et al., 2011). Erosion models have also been used and combined to fingerprinting with the same purpose. The different but complementary insights gathered by Palazón et al. (2016) combined the use of physiographic characteristics to address sediment yield's distribution and timescale, and fingerprinting added information on

sediment source contribution. Enabling the authors to derive information on mobilization and transfer capacity from source to sink.

As mentioned by Gentine et al. (2012) the scale of observation can be different from the scale of process modelling. So, a more accurate process representation should address the variabilities by coupling the analysis of these dynamic systems. While terrain analysis and erosion modelling address hillslope processes, sediment fingerprinting enlightens the connection between them and the drainage network. The integration of these approaches should improve the understanding of the erosive process from source to outlet of a catchment.

Concerning this, three environmentally fragile paired headwater catchment's, nested within Guarda Mor catchment, with intense agricultural use were subject to an evaluation of their erosive susceptibility and its spatial distribution. This study characterizes their fragility to the erosive process based on erosion modelling and their importance to the sediment discharge sampled at its outlet.

2 HYPOTHESES AND OBJECTIVES

2.1 HYPOTHESES

The connection between erosive processes observed over a hillslope and those observed on the drainage network (sediment yield) depends on sediment mobilization and transfer mechanisms from its sources to a catchment outlet. The coupling of results from a technique of sediment source identification with the estimate for erosion over a catchment will contribute to the improvement of both techniques.

2.2 OBJECTIVES

2.2.1 Main Objective

Analyze Guarda Mor upstream catchments' fragility to the erosive process based on topographic and erosion modelling and their relationship with sediment delivery.

2.2.2 Specific Objectives

Evaluate Guarda Mor upstream catchments' susceptibility to soil loss, surface runoff generation and sediment yield.

Identify the contribution of different potential sediment sources delivering sediments to the fluvial channel.

3 LITERATURE REVIEW

3.1 SOIL EROSION

Soil erosion is a natural process which can be enhanced by human disturbances on the environment. The process of soil erosion by water occurs in three phases, soil detachment, transport and eventual deposition (MORGAN, 2005). After detached, disaggregated particles may be transported by water that flows on the surface or can migrate through the soil's pores and cause its clogging, leading to surface crusting (MCINTYRE, 1958). Runoff's transport capacity may be increased by the amount of detached particles it carries, that promote turbulence in runoff and lead to rill erosion. Detachment by flow decreases as its sediment load increases (CAREY, 1984). Therefore, rates of detachment and deposition vary according to its sediment load and transport capacity. The detachment rate capacity is higher when sediment load is the lowest, and when sediment load equals transport capacity, deposition is nearly zero (FOSTER; MEYER, 1972).

Soil detachment, transport and deposition processes and mechanisms are complex. Thus, different scales are used to study different processes (GENTINE et al., 2012). On a catchment scale, the complexity from detachment to deposition can be considered, along with its interaction with the different landscape components. This reflects in the sediment load and characteristics delivered at catchment's outlet (MINELLA et al., 2010).

It is also on this scale that on and off-site erosion problems and damages can be accounted for. On-site, erosion degrades productive lands by decreasing soil's fertility, productivity and sustainability. While off-site transported particles cause water pollution and contaminant's transport. This may lead to reservoir and channel siltation, eutrophication, increasing floods, elevation of water treatment costs and overall ecosystem disruptions, resulting in a much higher cost of erosion off-site (PIMENTEL et al., 1995).

According to Julien (1995), deposited sediment on water channels reduce its transport capacity, which results in more frequent floods and damages to adjacent properties. These problems have been mentioned by Durlo and Sutili (2014) on Guarda Mor stream, in South Brazil. It has intense fluvial dynamics that have generated significant changes in its drainage network. The stream has been redesigned by material

being transported. The occurrence of overflows and floods caused structural problems on houses near eroded riverbanks, damage to roads, plantations and huge deposit mobilizations with large boulders.

Therefore, understanding and preventing erosion's negative effects is essential for soil and water conservation. For sustainable agriculture to be responsible for natural resources preservation, its planning must consider landscape analysis and its association to human activities. The need to understand and address this issue lead to the development of several models that consider the complexity of the hydrological and erosive processes on a catchment scale (SINGH; WOOLHISER, 2002). Models allow planning to be less expensive and time-consuming, especially since input data from remote sensing has become easily available. Elevation data has been used for modelling and spatial visualization of topography-controlled erosive and hydrological processes (MOORE; GRAYSON; LADSON, 1991).

Besides being a soil forming factor, topography exerts control on erosion. For instance, steep slopes are associated with higher erosion risks (GOLOSOV; WALLING, 2019). Topography and, consequently, hydrological processes cause variations in runoff and erosion in space and time, over hillslopes (HUANG; GASCUEL-ODOUX; CROS-CAYOT, 2002). Topographic characteristics have been associated with differences in runoff generation and hydrological responses in nested sub catchments (DIDSZUN; UHLENBROOK, 2008), as steep hillslopes promoted higher erosion vulnerability and sediment supply to rivers in headwater catchments (DUVERT et al., 2010).

A landscape's potential fragility is a natural vulnerability due to its physical characteristics, relief-governed, while an environmental fragility also considers the protection level given by land uses and cover to the environment (KAWAKUBO et al., 2005). According to Ross (1994), for environment planning, it is necessary to consider its fragility. The author proposes a methodology that empirically evaluates an environment's fragility based on its nature and human interventions. It considers the levels of protection given by vegetation or conservationist practices and levels of fragility considering, for example, soil types or slope range.

Topographic thresholds affect the severity and type of erosion processes (POESEN et al., 2003). Thus, different authors (CABRAL et al., 2011; LEPSCH, 2002; SANTOS; SOBREIRA, 2008; TROMBETA et al., 2012; BUITRAGO; MARTÍNEZ, 2016) point the importance of using terrain information on urban, environmental and agricultural planning for avoiding soil degradation and for protecting natural resources.

Complementary insights can be obtained by associating terrain to land use and soil surface characteristics in erosion modeling (NEARING et al., 2005; SIMONNEAUX et al., 2015), contemplating its spatial and temporal distribution. Further, sediments from soil erosion that reach river systems also provide information on its spatial sources that can be linked to the different processes that control erosion on a catchment scale (BOUDREAULT et al., 2019; KITCH et al., 2019) Integrating results that address different processes provides a holistic perspective of erosion on a catchment scale.

3.2 TOPOGRAPHIC ATTRIBUTES DETERMINATION ON EROSION ANALYSIS

The analysis of the landscape's geomorphology can be used in studies that address potential and environmental fragilities. The landscape variables that can be parameterized describe hydrological and geomorphological processes. Topography is one of the controlling factors on flow of energy and matter (water, nutrients, sediments and contaminants) over a terrain and hence, it controls soil water spatial variability (MOORE; BURCH; MACKENZIE, 1988), soil characteristics, erosive processes and soil and water degradation (MOORE; BURCH, 1986a, 1986c). Geomorphology influences surface runoff, because of this, geomorphological features are integrated to models that attempt to describe environmental processes (MINELLA; MERTEN, 2012).

Hydrology studies the movement, distribution and quality of water in the environment. Its movement though the landscape is controlled by gravity and relief components can modify it. This effect can be evaluated by digital elevation model (DEM) analysis, especially in environments where topography exerts greater effect on water movement. DEM analysis is a way of parametrizing phenomena related to an environment's hydrology (GRUBER; PECKHAM, 2009). All landscape components have ecological and hydrological importance and considering them is especially important for sustainable agricultural planning. This was made easier to accomplish with the development of Geographic Information Systems (GIS), by easily performing calculations, and with the available (and free of charge) elevation data for users (GRUBER; PECKHAM, 2009).

When quantifying topography's control over physical process, topographic indexes are used, as they characterize both simple and complex terrain attributes. Topographic indexes have been used in modelling of hydrological, geomorphological and

biological processes, since they are difficult to directly measure over large areas (MINELLA; MERTEN, 2012).

Some terrain characteristics are widely used in hydrological studies and have a strong connection with erosive processes governed by surface runoff. On Table 1, some of the main terrain characteristics related to runoff formation and erosive processes are shown. They are denominated topographic indexes and classified as primary and secondary. Secondary attributes are determined by the combination of primary, obtained directly from DEM.

Table 1 – Primary topographic attributes used for environmental fragility analysis.

Primary attribute	**Hydrological meaning**
Hypsometry	Climate, vegetation type, potential energy.
Slope	Surface runoff speed.
Profile curvature	Flow acceleration, erosion/deposition rate.
Plan curvature	Flow convergence/divergence, soil water content.
Slope length	Erosion rate, sediment yield, time of concentration.
Specific catchment area	Runoff volume, steady-state flow rate.

Source: Moore; Grayson; Ladson (1991), Moore; Gessler; Peterson (1993), Wilson; Gallant (2000).

Thus, inference on the location and magnitude of the erosive process on a catchment scale can be made (MOORE; GRAYSON; LADSON, 1991), for example: a) slope classes show the terrain's erosive capacity and are directly linked to runoff volume and speed; b) terrain curvature, in which profile curvature is used to characterize changes in flow speed and processes related to sediment transport, while plan curvature shows water's tendency to converge or diverge over a landscape.

Plan curvatures can be convergent, planar or divergent (negative, 0 or positive values), and profile curvatures, convex, linear or concave (negative, 0 or positive values). Over a convergent terrain, the directions of greater slope tend to converge, and the opposite on divergent ones, for this reason, this information is used to determine zones of higher or lower runoff incision on disaggregating soil particles and on sediment transport. Flow representation over different curvatures can be seen in Figure 1.

Soil water content, runoff's origin and acceleration are connected to terrain curvatures. Convex profile curvatures tend to create greater runoff speed and volume over the lower third of a hillslope, given the concomitance of greater slope length and

steepness, leveraging erosive process in those areas. When associated to convergent plan curvatures, the erosive potential is responsible for severe erosion.

Figure 1 – Representation of different terrain curvatures.

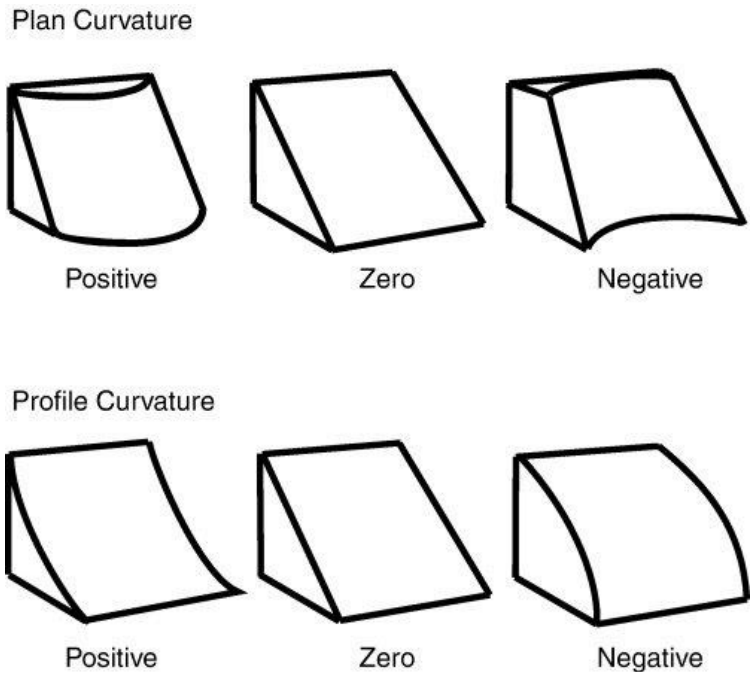

Source: Heine; Lant; Sengupta, 2004.

The hillslope's shape defines the contributing or catchment area, which corresponds to the amount of area over which water inputs can accumulate. From that, it can be derived the specific contributing area which refers to accumulated area per unit contour length. This primary attribute is combined with slope and provide different secondary attributes (Table 2) (GRUBER; PECKHAM, 2009).

Secondary attributes are used to indicate the spatial variability of areas with potential to accumulate water over the soil and, consequently, areas prone to runoff formation due to soil saturation and, also, sediment deposition (Topographic Wetness Index – TWI). As well as, the potential for flow concentration with greater speed, strongly related to sediment disaggregation and transport by runoff (Stream Power Index – SPI). There is also the Sediment Transport Capacity Index, which represents in a similar way the estimation for RUSLE's topographic factor, LS Factor, for zones of complex terrain.

The TWI, used on TOPMODEL hydrological model (BEVEN; KIRKBY, 1979; QUINN et al., 1995), describes the tendency of a cell to accumulate water. It is based on mass balance and considers the tendency of a cell to receive and hold water considering

the accumulated catchment area and slope. It is used for several terrain-related applications, such as the analysis of vegetation, soil properties, landslide initiation, hillslope hydrology (GRUBER; PECKHAM, 2009) and hydrological modelling (QUINN; BEVEN; LAMB, 1991). Soil saturation is a fundamental factor on soil erosion. In convergent planes, for instance, this causes surface runoff to concentrate and soil shear and detachment are favored. While higher TWI values may represent overland flow connectivity in a catchment, isolated areas of higher TWI are also representative of hydrological sinks and dysconnectivity, favoring sediment deposition (JANCEWICZ; MIGÓN; KASPRZAK, 2019).

Table 2 – Secondary topographic attributes.

Secondary attribute	**Meaning**	**Equation**
Topographic Wetness Index (TWI)	Characterizes the spatial distribution of saturation zones and landscape water content. It demonstrates the effects of terrain on location and extension of water accumulation areas. Digitally, it describes the tendency of a cell to accumulate water.	$TWI = \ln(Ac/\tan\beta)$
Stream Power Index (SPI)	Measures the erosive power of water flow. Predicts erosion on areas of convex profile (flow acceleration) and deposition on areas of concave profile (flow speed reduction).	$SPI = Ac.\tan\beta$
Slope Length and Steepness Factor (LS Factor)	This index measures the sediment transport capacity.	$LS\ Factor = (Ac/22.13)^{0,6} . (sen\beta/0,0896)^{1,3}$

* Where: Ac is the specific catchment area. β is the cell's slope. Ac is defined as the number of cells, or area, which contributes with the total water volume of a specific cell, it is the upstream accumulated area per unit width, transversal to the flow direction.
Source: Moore; Grayson; Ladson (1991), Moore; Gessler; Peterson (1993), Wilson; Gallant (2000).

The SPI represents the measure of flow erosive power, indicating runoff's erosive power over zones of concentrated flow. Water erosion on a catchment scale happens through many forms, diffuse and concentrated, but erosion models do not always account for all forms of erosion and are usually specific to one or two forms of soil erosion. For different soil and terrain conditions, some forms of erosion may be more important than others and some models might under or overestimate its results. Thus, the unit Stream

Power was developed by Bagnold (1966) (shear stress times flow velocity) and Yang (1972) (power per unit weight of water). It represents the time rate of potential energy dissipation per unit weight of water, or a measure of moving water's erosive power.

Because of difficulties in validating this concept in river systems, Moore and Burch (1986c) consider the application of this theory to an eroding area is physically more analogous, hence soil erosion could more successfully represented than its usual application to river and sediment transport studies. Besides studies on erosion and sediment yield, Stream Power is important for simulating preferential runoff channels, hillslope evolution and zero order basins formation. On environmental studies, modelling preferential channels is important to simulate pollutant and sediment routes and their connection to water bodies.

Moore and Burch (1986c) tested the hypothesis that the unit Stream Power theory can describe sediment transport capacity of interrill and rill flow, their results prove that this is a simple but robust method. According to Moore and Burch (1986a), this theory combined to a digital terrain model can be applied to describe the effects of the landscape on soil erosion and deposition zones. Measuring the Stream Power is difficult; therefore, a topographic index of stream power was developed by Moore; Burch; Mackenzie (1988) for estimating it with good precision (MINELLA; MERTEN, 2012). As the SPI describes potential flow erosion, with increasing catchment area and slope steepness, the amount of water and is flow's speed increases and, therefore, so does stream power and potential erosion (GRUBER; PECKHAM, 2009). Mhiret et al. (2018) found the SPI, and the TWI, to be good predictors for gully formation.

The topographic index that addresses sediment transport and surface flow over an area unit was derived by Moore and Burch (1986b) and Wilson and Gallant (1996). The parameters used for this relation are the same as for calculating the LS factor from the Universal Soil Loss Equation (WISCHMEIER; SMITH, 1978), but it also considers the shape of the hillslope. This physically based factor accounts for more complex landscapes. It can be used to indicate zones of erosion occurrence due to greater steepness and catchment area, resulting in greater sediment transport capacity, and representing the spatial distribution of potential soil loss (MINELLA; MERTEN, 2012).

Hence, the analysis of spatial data with geographic information systems proves to be a reasonable and inexpensive tool in predicting erosion where topography is a main controlling factor. Evidence regarding agricultural fields was found by Capoane et al. (2015) by a correlation between topographic attributes and soil chemical attributes in a

catchment in Júlio de Castilhos, Southern Brazil. The author found that the use of topographic attributes, calculated from high resolution DEMs, proved to discretize zones prone to material loss and deposition and can be used for estimation soil phosphorous and carbon concentrations.

Another research by Maestrini and Basso (2018) associated within field differences in the TWI to crop yields, in the US Midwest. The areas where neither too much runoff is formed nor water accumulates, mid to high TWI, are associated to high and stable yields, since there's greater water availability for plants. They also evaluated temporal variability and found that in areas that are prone to saturation (very high wetness index) have better performances in dry years.

Importantly, mapping these variables is part of the implementation of precision conservation (BERRY et al., 2003). It aims to address the natural variabilities of a landscape and to propose the most appropriate practices for soil and water conservation, by reducing environmental impacts of agriculture. Its applicability to catchment scales is key to identifying risk areas and maintaining natural resources and environmental sustainability (BERRY et al., 2005).

3.3 MODELING AS A TOOL FOR ASSESSING EROSION RISK

As previously mentioned, topographic attributes' analysis is a quick and useful tool for spatial representation of erosive processes associated to runoff formation for extensive zones of complex terrain. However, the erosive process is dynamic in time and dependent of other controlling factors. A more detailed analysis of an environment's fragility to erosion embodies rainfall characteristics and controlling factors such as soil type, land use and management. Hence, erosion mathematical models appropriate to catchment scales are used. It is important to highlight that for this scale, models must incorporate in their terrain components the hydrological concepts introduced in the previous item.

Models synthetize existent knowledge regarding a system or environment in equations that represent different processes and their importance concerning the problem (JOERGENSEN; FATH, 2011). So, for models to be effective in describing a natural system and phenomena representation, there must be scale compatibility and input data representativity for its adequate functioning (ROBERTSON et al, 2007). Besides, the

applicability of models arises given the amount, descriptive ability and difficulty level for parameter obtention. Usually, physics based, distributed models can describe detailed phenomena however (e.g. LISEM), the number of implicating parameters make numeric solutions for calibration and validation difficult. While some models require relatively fewer input parameters, making the numeric solution objective, yet with a limited process description (e.g. RUSLE).

Over the last years, many erosion models for catchments have been developed or advanced (MERRITT; LETCHER; JAKEMAN, 2003), becoming more accurate as computing systems have assisted and made modelling faster. Erosion modeling studies allow process description and prediction of how this dynamic is affected by system or environmental changes according to shifts in parameters and external variables, such as rainfall patterns (GOVERS, 2011) and/or land use and management. It is a helpful tool as for showing scenarios of potential soil erosion rates, its causes and, therefore, points areas vulnerable to soil erosion. The complexity of models varies according to the considered processes and data. Soil erosion models can be classified into empirical, conceptual or physics based. The choice of a model must be based on the purpose of use, the study site's characteristics and data availability (MINELLA et al., 2010).

The worldwide-used Universal Soil Loss Equation (USLE) is an empirical model that estimates the average rate of soil erosion per year. It combines the crop system, soil type, rainfall pattern and topography of a given plot. It is simple enough so there is no need for measured data as more complex models. It was originally developed at an agricultural plot scale in the United States of America (WISCHMEIER; SMITH, 1978), but it has been used in a range of areas of different terrains, land uses and climate. In these cases, results cannot be considered accurate and careful parametrization must be performed. Also, because of the scale it was developed at, the model doesn`t account for deposition nor sediment routing and transfer. Regardless of its uncertainty, modeled results can be taken as estimates (WISCHMEIER; SMITH, 1978) and they have been used as a means of identifying vulnerabilities (BENAVIDEZ et al., 2018) or erosion hotspots (CHANG; BAYES, 2013; TAMENE et al., 2017) on a landscape, generating erosion risk maps (LENCHA; MOGES, 2015).

Physics based models combine several equations that represent processes on a catchment scale. The Limburg Soil Erosion Model (LISEM) is a spatially distributed, event-based model that incorporates various processes in equations that describe hydrological and erosive processes in a catchment scale (DE ROO; JETTEN, 1999). It

was developed for planning and conservation and its results depend on quality and spatial resolution of GIS inputs. A different physics-based model is WEPP (FLANAGAN; NEARING, 1995), initially applied for assessing water erosion controlling mechanisms over hillslopes. Besides considering hydrological and erosive processes, plant growth process representation is an important segment of this model as it is considered to have large impact on the previous processes. Plant and residue characteristics are estimated daily, requiring extensive information. Its watershed version groups modelled hillslopes and links the results to the channel network, increasing the risks for accumulated errors. LISEM and WEPP require extensive data for model input and parametrization (MERRITT; LETCHER; JAKEMAN, 2003), therefore they have been used in long term monitored catchments (COCHRANE; FLANAGAN, 1999; BARROS et al., 2014).

Another raster-based spatially distributed and event-based model is the Surface and subsurface water and erosion modeling (WATERSED), developed to model the spatial distribution of runoff and erosion from field to catchment scale (0.01 to 1000 km^2). WATERSED is an upgrade of the Sealing and Transfer by Runoff and Erosion related to Agricultural Management (STREAM) model (LANDEMAINE, 2016). STREAM was developed to avoid over-parameterization and uncertainties in modelling (CERDAN et al., 2002).

Evrard et al. (2009) found STREAM to be efficient for predicting runoff convective storms, rather than events of low intensity, and satisfactory in predicting runoff and erosion when/where hortonian overland flow is a dominant process. STREAM was also used by Delmas et al. (2012) to quantify runoff and erosion's scale effect from hillslope to catchment, and for assessing runoff and interill erosion.

These models combine parameters in expert-based decision rules as tables, combining land use, soil type and their corresponding field-based information, such as the parameters soil crop cover, surface state, roughness and moisture from previous rainfall. Then, they are combined and a steady-state infiltration rate for each cell for a rainfall event is assigned (Figure 2).

In the model's hydrologic module (LANDEMAINE, 2016), the hydrologic balance of each cell is calculated for a given rainfall. Flow velocity is calculated for each cell and channels, from it travel time is computed. Runoff duration is used for addressing re-infiltration and flow routing is given according to two algorithms, depending on local slope. From this module, runoff peak ($m^3\ s^{-1}$) is obtained.

Figure 2 – Conceptual model of the infiltration/runoff balance assessment module.

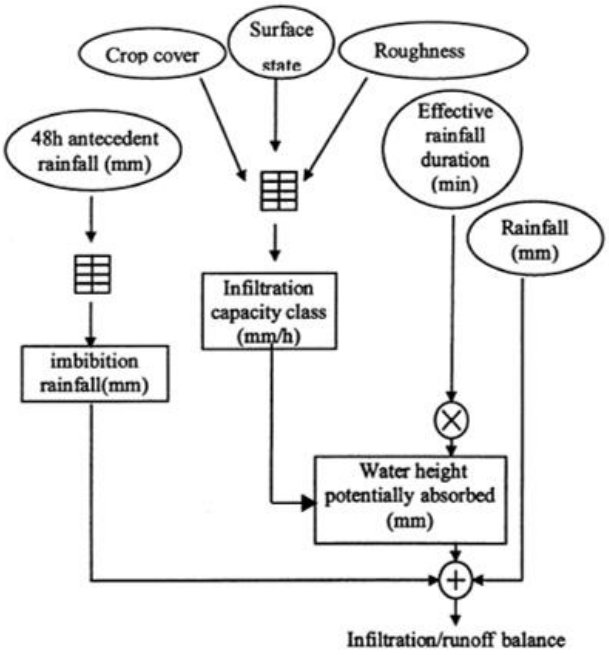

Source: Cerdan et al. (2002).

The sediment module (LANDEMAINE, 2016) considers topography, soil surface and rainfall characteristics for interrill and concentrated erosion generation. A potential sediment concentration value is set in one of the tables and is used for calculating interrill erosion. Sediment is transported by runoff, proportionally to its volume; and deposition occurs when sediment transport capacity is exceeded. After reaching the river channel, sediment is transported downstream and riverbank or channel erosion are not predicted by this model.

Overall, spatially distributed modelling approaches are adequate for understanding sediment transport, since every sediment source is characterized by different travel times (MERRITT; LETCHER; JAKEMAN, 2003). And considering the potential difficulties in representing processes or the need for interpreting physical phenomena with equations and parameters without overloading model parametrization, WATERSED seems to have the attributes for overcoming these features. Thus, the obtained results hold the advantage of its use in resource management and for phenomena descriptive interpretation.

3.4 SEDIMENT YIELD AS AN INTEGRATING ELEMENT OF THE EROSIVE PROCESS IN A CATCHMENT

Studies on sediment yield provenance and transfer are fundamental for comprehending the erosive processes in a catchment scale. This information is necessary for evaluating the offsite impacts of erosion, for water resources management (MINELLA; WALLING; MERTEN, 2014) and for modelling calibration and validation. It is also useful to propose effective strategies for controlling sediment yield (WALLING; OWENS; LEEKS, 1999; WALLING, 2005) and to optimize resource application on soil and water conservation practices.

The complexity of processes and parameters that regard hillslope and bank erosion makes it difficult to quantify sediment supply from a catchment to a river channel (JULIEN, 1995). Methods used to understand suspended sediment sources face difficulties since the factors governing sediment mobilization and delivery vary in space and time. To address this, an important monitoring strategy has been developed that is the coupling between traditional sediment monitoring programs associated with tracing techniques (COLLINS; WALLING, 2004). Evrard et al. (2011) found this combination to improve the understanding of the erosive processes and their diversity within a catchment.

Over the last decades, sediment tracing has been developed for understanding sediment sources (PEART; WALLING, 1986). Huon et al. (2017) found that the contribution from surface and subsurface sources to be dominant in upper and lower parts of a catchment, respectively. The authors were able to infer on rainfall event's characteristics, land use and connectivity as controlling factors for suspended sediment's sources. Furthermore, sediment fingerprinting combined to catchment erosion modeling enhanced knowledge and provided complementary insights on erosive processes and river transport capacity (PALAZÓN et al., 2016).

The fingerprinting approach (Figure 3) is based on the premises that: a) sediment has different parameters or fingerprints that can be used to distinguish its source, b) the comparison of suspended sediment and samples from soil sources allows the distinction of sources contributions to sediment load, and c) the desirable tracing properties for sediment are constant in space and time (HADDACHI et al., 2013). These tracer discriminant characteristics are due to geology, soil management, depth of the erosion

process and terrain wetness, which are responsible for soil differences and consequently, eroded sediments.

Therefore, it is possible to determine potential sediment of either spatial sources or source types, as the nature of the main sediment sources operating within a catchment through fingerprinting (WALLING; WOODWARD, 1995). Spatial sources can be based on sub basins, geology or soil units while source types may be land uses or different erosive processes, such as surface or subsurface (COLLINS; WALLING, 2004).

Figure 3 – Conceptual model of sediment tracing.

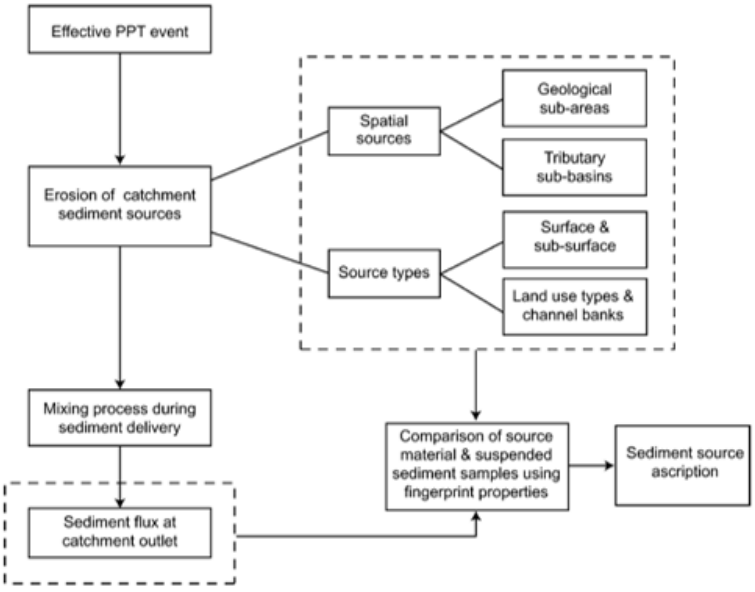

Source: Collins and Walling (2002).

There are different methods for analyzing samples in order to trace its source. Usually, geochemical composition and fallout radionuclides are used, but other tracing properties have been used over time: magnetic susceptibility, stable nitrogen and carbon isotopes, mineralogy and recently color and spectroscopic analyses. Geochemical and radionuclide analysis require laboratory equipment and several analyses that make this an expensive and time-consuming procedure. On this approach, the discrete variables obtained for each sample are submitted to a set discriminant analysis as Kruskal-Wallis test and a multivariate discriminant function analysis based on the minimization of Wilk's Lambda to identify the most significant set of parameters. Then, a multivariate mixing

model is used to estimate the sources' relative contributions (COLLINS; WALLING; LEEKS, 1996).

According to Walling (2013), many fingerprinting studies involve much trial and error; also, extensive initial analyses are made, depending on available equipment, and only later they are statistically tested for its discrimination properties. Given this, many researchers have been striving to fingerprint source materials and sediments with alternative tracers, from time-efficient and cheaper methods. Alternative methods should allow for a large number of samples to be analyzed without extensive laboratory preparation.

A physical analysis of dried sieved samples, spectroscopy, was shown to be useful to characterize soil properties. Viscarra Rossel et al. (2006) used diffuse reflectance spectroscopy analysis on the visible (VIS), near infrared (NIR), mid infrared (MIR) and combined spectra ranges to obtain qualitative soil interpretations from the soil spectral bands and to quantify soil properties. The statistical procedure differs, since the data consists of several wavelengths, a much larger number of variables compared to the conventional approach. The authors performed property prediction using a Partial Least Squares Regressions (PLSR) model, for multivariable data analysis. This less expensive and non-destructive analysis, that also requires smaller amounts of samples (MARTÍNEZ-CARRERAS et al., 2010c), was then tested for its potential to discriminate source materials.

Poulenard et al. (2009) demonstrated the potential of Diffuse Reflectance Infrared Fourier Transform (DRIFT) spectroscopy in the MIR range to trace sediment in a small watershed. Their results showed the approach's potential for discriminating sources, as it is both relatively simple and cheap to use. Supporting that, Brosinsky et al. (2014a) and Martínez-Carreras et al. (2010b) found spectral fingerprint analysis to be rapid, cost-efficient and non-destructive. In South Brazil, MIR (TIECHER et al. 2017), NIR (TIECHER et al. 2015) and UV-VIS spectroscopy (TIECHER et al. 2016) were proved to be successful in order to characterize source materials and sediments. Regarding the conservativeness of source material's properties, Poulenard et al. (2012) demonstrated that submerged samples' DRIFTS signature was sufficiently conservative for its use as a fingerprinting property.

Studies have used spectroscopy to quantify sediment sources by means of deducing color coefficients from spectra (MARTÍNEZ-CARRERAS et al., 2010a; MARTÍNEZ-CARRERAS et al., 2010c, BROSINSKY et al., 2014b, BOUDREAULT et

al., 2018, EVRARD et al., 2019) or predicting concentrations of geochemical properties to be used as fingerprinting properties (MARTÍNEZ-CARRERAS et al., 2010b) and then applying a mixing model, and directly using the spectra to estimate the proportion of source materials and using a PLSR calibration with artificial mixtures (POULENARD et al., 2009, POULENARD et al., 2012, EVRARD et al., 2012, LEGOUT et al., 2013, VERHEYEN et al., 2014, TIECHER et al., 2015). These mixtures were used to construct PLSR models and to quantify the proportion of different source materials in suspended sediment (POULENARD et al., 2012). The models built for each sediment source attempt to find a linear relationship between the spectral dataset (x variable) correlate to a proportion of sediment contribution (y variable), calibrated with the artificial mixtures.

A PLSR is usually used when the variables present high collinearity. This algorithm maximizes the covariance between the spectra and the artificial mixtures used for calibrating the models. A limited number of factors are responsible for explaining the variations in predictor and depended variables (WOLD; SJÖSTRÖM; ERIKSSON, 2001). While the mentioned sediment source apportionment studies used PLSR to develop models for sediment source prediction, for soil properties' prediction, another (and more recent) regression called Support Vector Machine (SVM) allows handling nonlinearity of spectral data (VISCARRA ROSSEL; BEHRENS, 2010).

SVMR differs from PLSR by being based on statistical learning theory. It maps X from given data put into a high dimensional feature space defined by a kernel function (KARATZOGLOU; MEYER; HORNIK, 2006). A kernel is a function that given two patterns returns a real number characterizing their similarity (SCHOLKOPF; SMOLA, 2001). The decision function is a kernel expansion corresponding to a separating hyperplane in the feature space (SCHOLKOPF; SMOLA, 2001). Boundary samples, the so-called support vectors, determine the separating hyperplane. For Viscarra Rossel and Behrens (2010), SVM was the best performing model for predicting soil organic carbon, pH and clay content. SVM models also had the best performance for predicting total carbon on soil samples, according to Lucà et al. (2017).

4. ARTICLE

Introduction

Soil erosion is responsible for damages of economic, social and environmental orders both on and, especially, off-site (Boardman et al. 2019). Eroded sediments carry pollutants, contaminants and nutrients (Yang et al. 2017) that lead to soil and water degradation. The controlling factors of erosion dictate the susceptibility of soils to this process (Morgan 2005). Soil and water movement over the landscape and its fragility regarding degrading processes are controlled by topography in South Brazil. Therefore, spatial prediction of erosion and its associated impacts can be obtained by analyzing this factor (Minella and Merten 2012).

Geomorphological parameters, or topographic attributes, obtained from digital elevation maps (DEM) are used in hydrological and, hence, erosive spatial representation (Gruber and Peckham 2009). Terrain analysis is applicable in soil classification and mapping (McBratney et al 2003), prediction of soil attributes (Moore et al. 1993), environmental planning (Ross 1994), precision conservation (Berry et al. 2005), determining erosion susceptibility (Vijith and Dodge-Wan 2019), risk (Buitrago and Martínez 2016) and hotspots (Mhiret et al. 2018).

Erosion models incorporate these landscape features to other parameters controlling erosion processes (Merritt et al. 2003). Runoff is an active agent in soil erosion and some models require greater data input for process simulation. While others, although simple, are robust in reproducing erosion and runoff dynamics satisfactorily. Dynamic and spatially distributed representations portray mass movement and process connectivity between hillslopes and the drainage network, providing adequate estimates for different scenarios. Added to topography features, WATERSED (Cerdan et al. 2002a; Cerdan et al. 2002b; Landemaine 2016) uses a simple parameterization for soil surface characteristics considering that they describe, at a catchment scale, infiltration and, therefore, runoff and erosion (Le Bissonnais et al. 2005).

Although sediment yield reflects the erosive processes of a catchment, material transfer from hillslopes to river systems depends on landscape connectivity and depositional processes (WOHL et al., 2019), affected and evaluated by geomorphologic characteristics (Jancewicz et al. 2019). Therefore, for targeted management, it is important to identify these sediment sources. Sediment fingerprinting studies (Walling

2013) allow for source type discrimination based on sediment and soil properties. Recently developed, simple and alternative ways such as near-infrared spectroscopy coupled to statistical modelling is efficient in estimating sediment sources (Verheyen et al. 2014; Tiecher et al. 2015).

Accelerated erosion processes, which have been causing floods and damages to the drainage network of a stream such as Guarda Mor (Durlo and Sutili 2014), can be mitigated by targeted sustainable management, benefiting soil and water environments. This study aims to integrate complementary tools for identifying such spots and for simulating soil and water's susceptibility to the processes controlling their degradation. Tools which should coherently address geomorphology, associated to upstream erosion modelling and the sediments found by the river system.

Material and methods

This study's methodology comprises three work packs in a complementary and integrated way. First, topographic attributes derived from DEM were analyzed to identify the sites fragile to erosion based on topography, then the erosive process was modeled with a physically based model to add the influence of others factors (climate, soils and land use) and last, sediment sources were estimated to compare with the previous analyses.

In the first work pack (WP1), data of primary and secondary topographic attributes were acquired for the set of sub catchments and main catchment under study. This approach spatially identifies the main hotspots where the erosive processes are heavily relief-influenced. For the second work pack (WP2), the erosive potential is considered from a more complex approach, by adopting a mathematical model that takes into account the hydrological and erosive processes. This is a dynamic method of evaluating soil fragility to erosion, using data on rainfall, land use, soil management and relief. Results from both techniques allowed demonstrating the spatial environmental fragility based on erosive process using two different levels of information and techniques.

Next, work pack 3 (WP3) addressed the origin of the suspended sediment, determined by means of the fingerprinting technique (Poulenard et al. 2009; Tiecher et al. 2016). The method seeks to integrate the erosive processes modeled in the hillslopes and sub catchments with the sediment yield observed in the main catchment. Different source groupings (land use and sub-catchments) were considered as endmembers to

analyze the spatial variability and the main processes related with the sediment yield. The fingerprinting approach integrated and allowed verifying the results obtained from the previous work packs. Ultimately, the analysis of these work packs identified the spots more susceptible to water erosion, their relationship with sediment yield and their connectivity to the drainage network.

Study area characterization

The study was carried on three headwater sub catchments of Guarda Mor catchment (Figure 4). This catchment is characterized by different land uses, soil types, rugged terrain and diverse geology. It is located within the limits of Ivorá, Silveira Martins and Júlio de Castilhos, in Rio Grande do Sul, Brazil. This stream drains to Soturno River, a tributary of Jacuí River, main contributor to the Guaíba Lagoon.

Figure 4 – Digital elevation map of Guarda Mor's main monitoring station **(**GMex), highlighting the headwater three sub catchments.

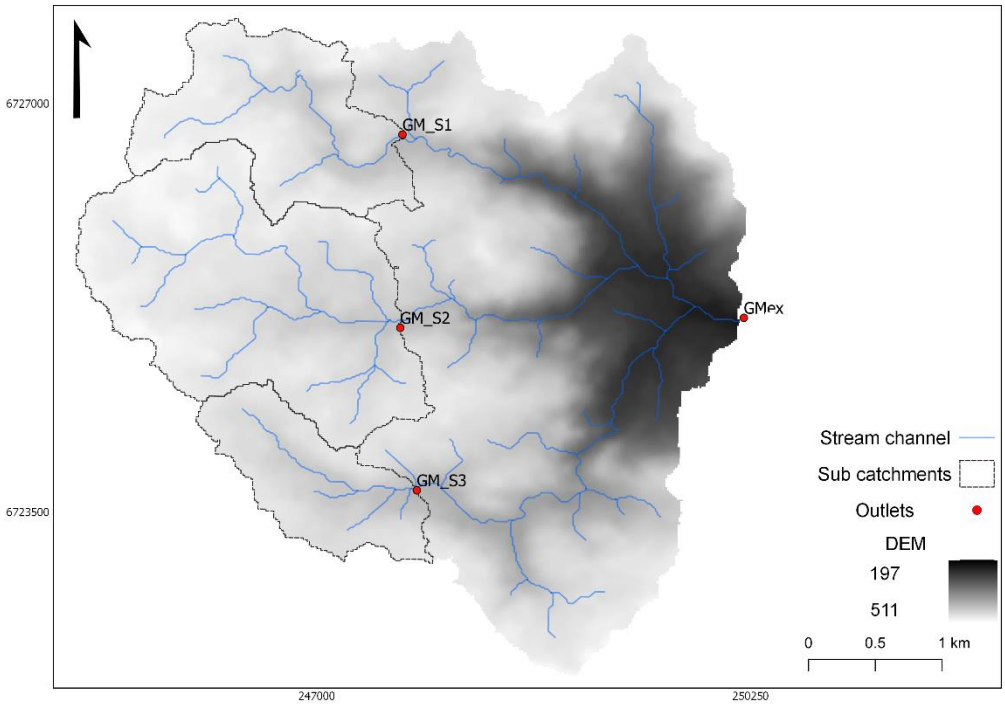

Source: Author.

Climatological data point to an annual precipitation regime of 1700 mm. The region's climate is subtropical, type Cfa 2, according to Köppen's classification, and the mean annual temperature is of 19°C (Durlo and Sutili 2014).

GMex has a drainage area of approximately 18.5 km² and elevation ranges from 197 to 511 meters (Figure 5). It is in a transition between the Meridional Plateau and Central Depression of Rio Grande do Sul. Planar to very undulating relief is observed in its upper and lower segments, while its middle third is characterized by an escarpment, a transition area of steep slopes. This catchment encloses three sub basins with drainage areas of 2.1, 4.2 and 1.4 km² each, henceforth called S1, S2 and S3, respectively.

Figure 5 – South American continent, highlighting Soturno, Guarda Mor and GMex catchments. Digital elevation map for GMex.

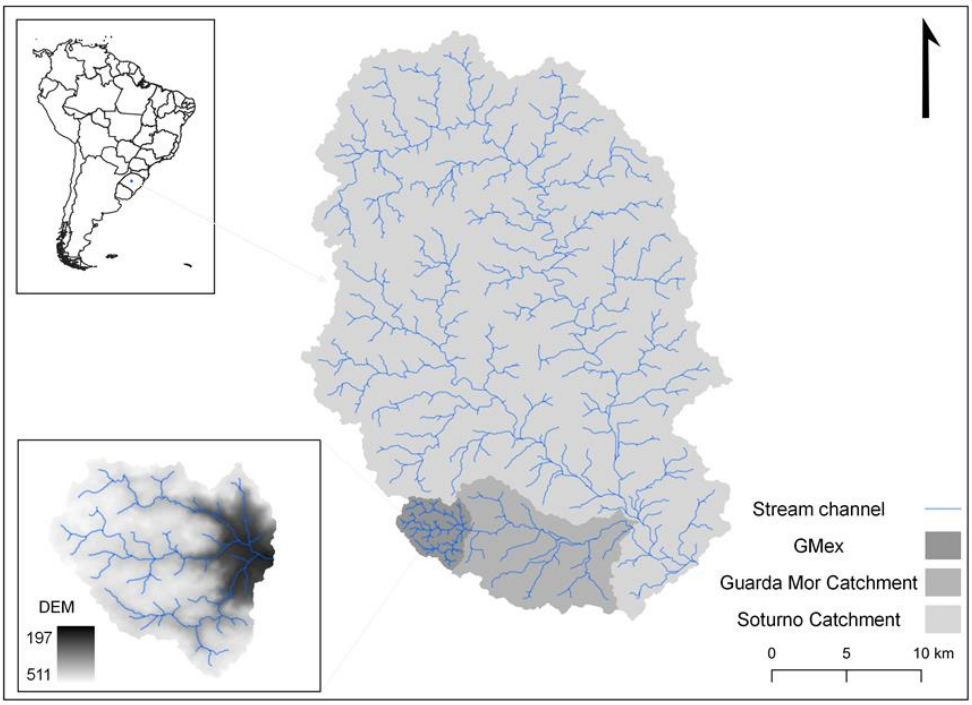

Source: Author.

This segmentation is represented by this catchment's diverse geology (CPRM, 2013) (Figure 6). The upper segment, comprising the Plateau, has volcanic rocks from the Serra Geral Formation, separated in the Caxias unit (rhyodacite), accounting for an

area of 1222 hectares (ha) and the Gramado unit (basalt) accounting for 396 ha of the catchment's middle third. In the Central Depression (sedimentary basin) predominate the sandstones from Botucatu and Caturrita Formations, where the Botucatu (fine sandstone), comprises 216 ha and Caturrita (sandstone) comprises 14 ha.

Figure 6 – Geology representation of GMex catchment.

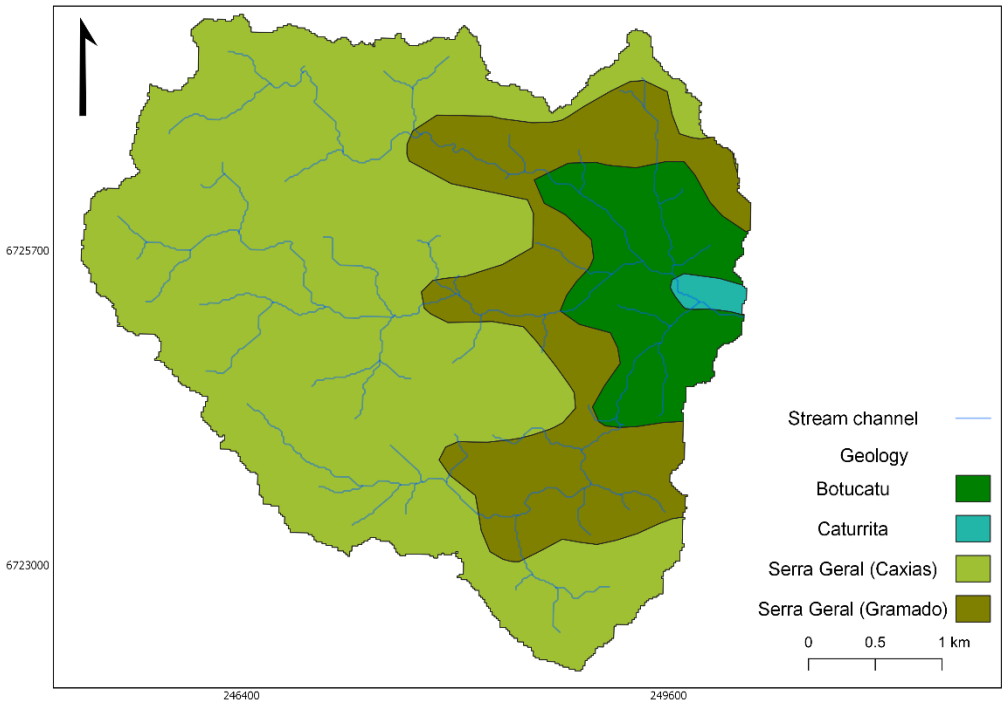

Source: Author.

By the Plateau, slope is predominantly undulating (slope between 5 and 10%), moving to very steep terrain (slope above 75%) in the middle third, and by the lower portion of this catchment, terrain varies from flat (slope from 0 to 2%) and undulating to very undulating (15 to 45%). Predominantly, the observed soil types (Figure 7) are Neossolos Litólicos, as classified by the Brazilian System for Soil Classification (Santos et al. 2018). These are shallow and less developed soils, which may present lithic material within 50 cm from the surface (Santos et al. 2018). Other observed soil classes are Nitossolos Vermelhos, well weathered and developed soils, well drained, with a slight clay-enrichment in its subsoil horizon (Santos et al. 2018). There are also small areas of Cambissolos Háplicos, less developed soils, by the Plateau. And Gleissolos Háplicos, soils which suffer reduction processes, are found near the streams in S2.

In the transition area of basaltic escarpment, the predominant soil classes are Neossolos Líticos and Regolíticos. Different from Neossolos Líticos, Neossolos Regolíticos should not present lithic material within 50 cm from the surface (Santos et al. 2018). By the lower segment of this catchment, there are Neossolos Litólicos and areas of Argissolos Acinzentados, which are deep, weathered and poor drained soils, with a characteristic clay-enriched subsoil horizon, formed by pedogenic processes such as clay migration (Santos et al. 2018). These soils classes should, closely, correspond to Acrisols (Argissolos), Cambisols (Cambissolos), Gleysols (Gleissolos), Nitisols (Nitossolos), Leptosols (Neossolos Litólicos) and Regosols (Neossolos Regolíticos) in the World Reference Base for Soil Resources (IUSS Working Group WRB 2015).

Figure 7 – Soil type representation of GMex catchment.

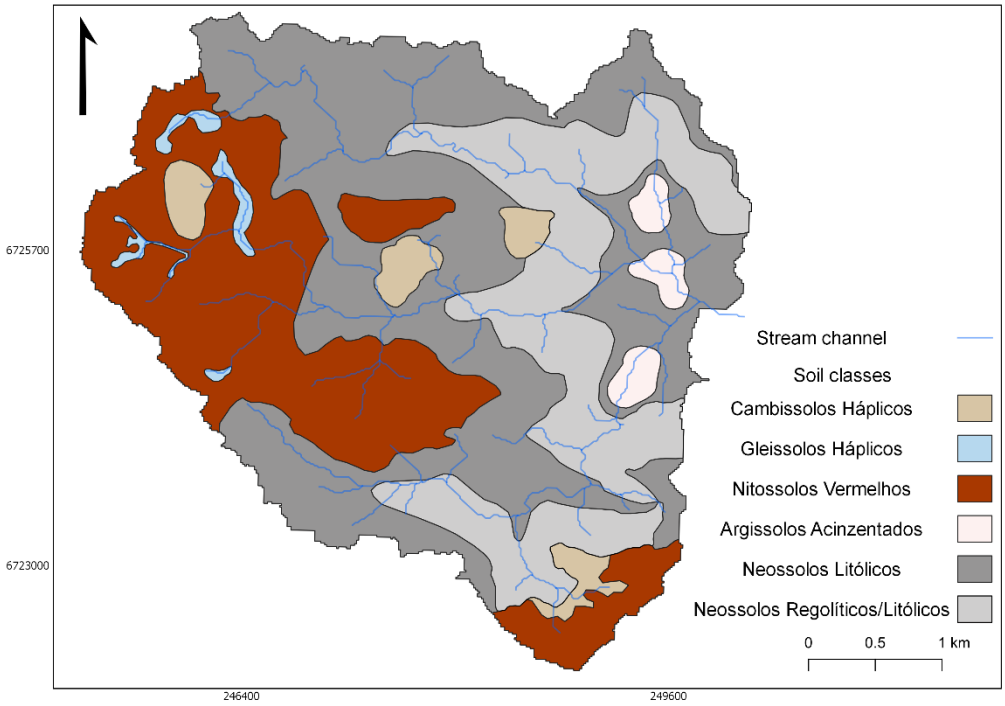

Source: Guarda Mor catchment's Soil Survey Report (UFSM's Pedology Group, in press)/ *Relatório do Levantamento de Solos da bacia do Guarda Mor (Grupo de Pedologia da UFSM, no prelo)*

Based on normalized difference vegetation index (NDVI) and field verification, a map of land use classification was built (Figure 8). The NDVI was derived from LANDSAT satellite images. According to this classification, approximately 43% of this catchment's land is occupied by forests, followed by cropfields (41%), grasslands (11%), urban or pavement areas (2%) and water bodies (1%), besides the area occupied by stream

channels. Forest, the main landscape component, is mostly located in the escarped region of this catchment. While in the upper segment, over the headwater catchments, land use is mainly of cropfields, in a no-till system, consisting of a binomial of summer soybeans monoculture and wheat or oats during the winter. Grasslands are areas of permanent pasture, without soil mobilization or seasonal crops.

Figure 8 – Land use representation of GMex catchment.

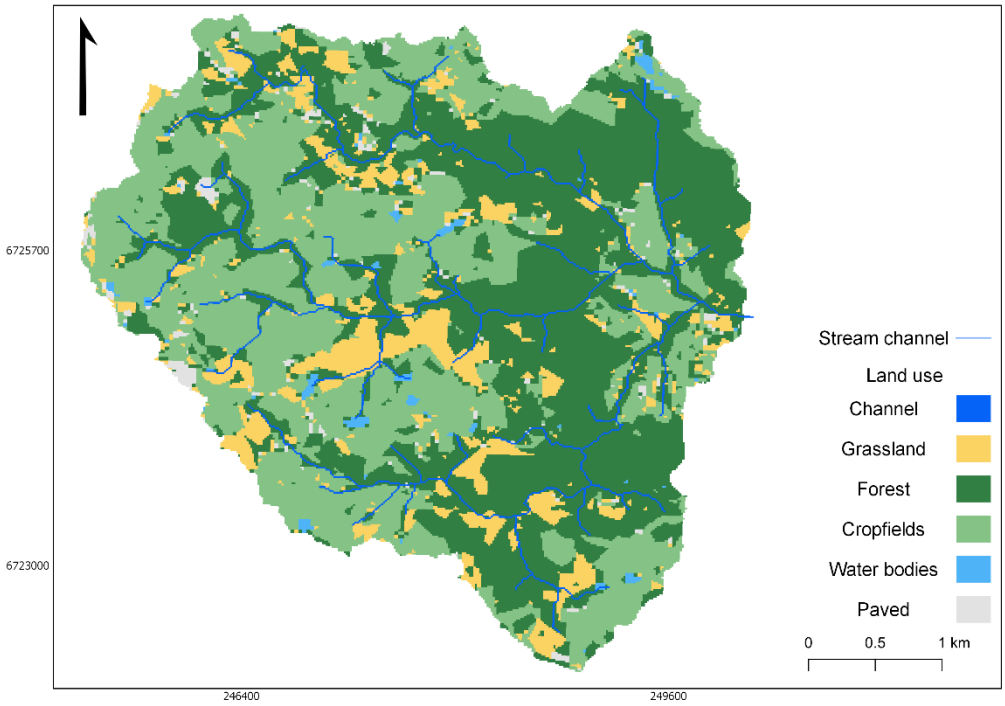

Source: Author.

Regarding the sub catchment's land use characterization, S2 and S3 are very similar, with an area of 62 and 63% occupied by cropfields, respectively. Forests occupy 20% on both catchments and 11 and 12% by grasslands. S2 has 2% of its area occupied by urban or pavemented areas, mainly farmhouses, which correspond to 0.1 km². S1 has a different occupation ratio. Although cropfields are also the main type of land use (45%), forests occupy 33% and grasslands 17% of this catchment's area.

Terrain analysis – Work pack I

An ALOS PALSAR digital elevation map (DEM) was obtained. Spatial resolution of this morphometric variable is of 12.5 m, having been interpolated to 15 m for this study. All maps were processed and obtained using the geographic information system SAGA GIS 2.3.2.

From input data DEM, primary topographic attributes, representing geomorphometric attributes, were obtained: a) slope, profile and plan curvatures were calculated by the method of the 9th parameter 2nd order polynom (Zevenbergen and Thorne 1987); and b) catchment area was obtained by using a recursive function.

Slope influences runoff velocity and it is a controlling factor of erosion and other geomorphic processes. Terrain curvature affects flow over a terrain and, consequently, erosion and deposition. Zero value for profile or plan curvature indicate linear or planar surfaces, respectively. Negative profile curvatures represent convex surfaces and positive, concave. Plan curvatures represent surfaces of convergent (negative values) or divergent (positive values) flow. Catchment area refers to the amount of runoff that may accumulate to a given point.

Slope and catchment area were then the input data used for calculating topographic indexes. They are the: a) Topographic Wetness Index, following Beven and Kirkby's (1979) TOPMODEL; b) LS Factor, based on the method of Moore et al. (1991); c) and the Stream Power Index, also based Moore et al. (1991). Later, QGIS 3.8.3 was also used for organizing and representing the final maps.

The wetness or amount of water a cell can accumulate is calculated in the TWI from catchment area and its slope. The LS Factor combines the effect of slope length and steepness in a potential capacity of accumulated runoff to cause concentrated erosion and transport sediment. And the erosive power of runoff is measured by the SPI.

Erosion modelling– Work pack II

WATERSED (Landemaine 2016) was used for modeling surface runoff and sediment yield of the three sub catchments. It is a simple, event and raster-based model that was developed for agricultural hillslopes and catchments. Its expert-based approach integrates dominant factors of soil erosion from information on soil type, surface, cover and rainfall characteristics to result in infiltration rates.

Its consistent conceptual structure includes both a hydrologic and a sediment module. First, in the hydrological module, the condition of each cell (i) is given by its hydrological balance (HB_{Ri}), in mm, for a rainfall event:

$$HB_{Ri} = R_i - IR_i - (\theta . IC_i . t_{effi})$$

Where R_i (mm) is the rainfall volume, IR_i (mm) is the amount of precipitation needed to reach soil saturation, IC_i (mm h^{-1}) is the infiltration rate, in steady-state, and t_{effi} the rainfall duration (min). The adjustment parameter θ was introduced to WATERSED so variations to infiltration rate from expert-judgement can be established.

From excess precipitation, E_{R_i} (mm or m^3), the average excess rainfall intensity, e_i (mm h^{-1}) is derived:

$$e_i = \frac{E_{R_i}}{t_{effi}}$$

Using Manning's formula for travel time, overland flow velocity V_{H_i} (m s^{-1}) is calculated:

$$V_{H_i} = \frac{S_i^{0.3} L_i^{0.4} e_i^{0.4}}{n_i^{0.6}}$$

S regards i's surface slope, L is i's flow length, and n is Manning's roughness coefficient (s $m^{-1/3}$). In V_{H_i}, important information regarding land use and excess rainfall are introduced and added to topographic features, along with the spatial variability they promote.

Then the equation for the channel flow velocity, V_{C_i} (m s^{-1}), combines Manning's and a steady state continuity equation for a wide channel:

$$V_{C_i} = S_i^{0.3} \left(\frac{Q_i}{W_i}\right)^{0.4} n_i^{-0.6}$$

Q (m^3 s^{-1}) is i's cumulative discharge from upstream flow and excess rainfall contributions, and W is the channel's width in meters. From dividing travel distance by V_{H_i} and V_{C_i}, travel time for i is calculated.

A triangular unit hydrograph describes flow through i during runoff. Upslope travel time, weighted by cumulative discharge, adds up to the lag time L_i (h). The centroid for effective rainfall, which is equally distributed over time, corresponds to $t_{effi}/2$. So, time to peak T_{P_i} (h) is the sum of L_i and $t_{effi}/2$. Then, runoff duration, or time of concentration T_{C_i} (h) is derived from T_{P_i} and a recession parameter, α:

$$T_{C_i} = T_{P_i} + \alpha . T_{P_i}$$

This recession parameter was introduced for adjusting re-infiltration; therefore, re-infiltration is based on T_{C_i}.

Flow is routed by two flow direction algorithms depending on slope value. If the value is lower than 2%, flow is routed by Multiple Flow Direction algorithm, which allows flow to diverge over large flat areas. If the value is greater than 2%, the algorithm Single Flow Direction is used, considering that flow concentrates in a single width cell.

The balance for runoff and infiltration, which leads to the accumulated water volumes, considers the runoff flow network. i can re-infiltrate part or all runoff generated upstream. This hydrological balance is calculated two times, one at the beginning of the simulation and also during flow routing.

Runoff peak Q_{P_i} ($m^3\ s^{-1}$) is calculated by using total runoff volume V_i (m^3) and runoff duration, assuming a triangular unit hydrograph:

$$Q_{P_i} = \frac{2V_i}{T_{C_i}}$$

The other element from this model's conceptual structure is the sediment module. It is assumed that topography, soil surface and rainfall characteristics are governing factors for interrill and concentrated erosion. For instance, the model uses E_{R_i} and a value for potential sediment concentration SC_i ($g\ L^{-1}$), assigned for each combination of soil surface characteristics, to calculate interrill erosion SE_{S_i} (kg):

$$SE_{S_i} = E_{R_i}.SC_i$$

Considering that on a catchment scale, transported sediments are proportional to runoff volume, the mass of sediment leaving i that produces runoff, SY_i (kg), is calculated by:

$$SY_i = SY_\alpha + SE_i$$

SY_α (kg) is the sediment mass from upslope cells and SE_i (kg) is gross erosion, or the sum of interrill and gully erosion. SY_i differs if sediment deposition occurs. This can happen due to the re-infiltration, where the mass of deposited sediment, SD_i (kg), corresponds to the re-infiltrated volume, I_i (m^3), and the flow's average suspended sediment concentration, $\overline{SC_\iota}$ ($g\ L^{-1}$):

$$SD_i = I_i.\overline{SC_\iota}$$

$$\overline{SC_\iota} = \frac{SY_\alpha}{Q_\alpha}$$

If so:

$$SY_i = SY_\alpha + SD_i$$

Or, sediment deposition occurs if $\overline{SC_i}$ exceeds suspended sediment concentration for the sediment transport capacity, SC_{TCi} (g L^{-1}). Then:

$$SY_i = Q_i + SC_{TCi}$$

Q_i (m^3) corresponds to runoff volume leaving i. The deduction of SD_i is given by:

$$SD_i = SY_a + SY_i$$

SC_{TCi} weighs $\overline{SC_i}$ by a ratio between Manning's roughness coefficient, which represents the hydraulic resistance promoted by vegetation, and i's submergence, by mean water depth h_i (m):

$$SC_{TCi} = \overline{SC_i}.exp\left(-\beta.\frac{n_i}{h_i}\right)$$

β corresponds to a decay parameter, and h_i equals to:

$$h_i = \frac{Q_i}{T_C.A_i}$$

Where, A_i is the contributing area (m^2).

Runoff and sediment that reaches the rivers are directly delivered to the lowest point downstream of the river. In this model, riverbank erosion and storage within the channel are not simulated. More detailed model description on equations, including for gully erosion, can be seen in Landemaine (2016). The equations that compose this model address the concepts of intrinsic soil vulnerability by its topography, while incorporating the properties of soil type and land use which can alter that environment's susceptibility to erosion. They require data for parametrization that can be easily obtained in the literature when the purpose of modelling is to estimate susceptibilities. This simple yet consistent structure makes it, by these means, a robust model.

The model works on SAGA GIS and the input data set is composed of tables and raster maps. These maps correspond to: DEM, used for extracting slope and water flow; stream network and channel width; soil type and land use. The land use map also accounts for landscape components such as stream channels, water bodies, urbanized areas and forests, besides grasslands and cropfields. Each land use is then associated to soil characteristics from decision tables. These were adjusted to local conditions, according to each land use or landscape component, in order to associate field observed soil properties to infiltration rate. They include values for: Manning's roughness coefficient, a potential value for sediment concentration, soil erodibility (Table 3) and antecedent

moisture content (Table 4). As for rainfall events, they were chosen from a monitored precipitation time series and correspond to rainfall depth and duration.

Table 3 – Expert table for land use characteristics.

Land use	Infiltration	Manning's n	MES	Erodibility
Grasslands	20	0.2	0.5	0.1
Forests	50	0.4	0.2	0.005
Cropfields	30	0.3	0.5	0.6
Water bodies	2	0.01	0.1	0.05
Paved/Urbanized	2	0.02	0.1	0.05

So far, there have been no field measured data for this catchment. Therefore, some parameters have been defined based on literature data or measured/modeled parameters from a field-scale, rainfall-runoff monitoring station in Júlio de Castilhos (Londero et al. 2017). Parameters (infiltration, suspended sediment concentration and erodibility) regarding agricultural land use were used since both areas present similar edaphoclimatic conditions. Climate in Júlio de Castilhos is also classified as Cfa. The monitoring station is also located on the Plateau. Its soils are deep and weathered, over undulating relief. They were formed over volcanic rocks (Londero et al. 2017), the same parent material present in the sub catchments. These characteristics make this site representative of Guarda Mor's headwater sub catchments.

Table 4 – Expert table for imbibition.

Infiltration	ANT0	ANT1	ANT16	ANT40
80	22	17	14	10
60	21	16	13	9
50	20	15	12	8
40	19	14	11	7
30	17	13	10	6
20	15	12	8	5
15	14	10	7	4
10	12	8	5	3
5	8	5	3	1
2	5	2	1	0
1	2	1	0	0

0	0	0	0	0

Values for Manning's roughness coefficient were chosen based on Engman (1986). Default scale effect correction and recession time, flow width, critical runoff peak for rill erosion and sediment settling parameter coefficients were applied. Three rainfall-runoff events monitored in Júlio de Castilhos were chosen to be modeled (Londero et al. 2017). Their characteristics are described in Table 5.

Reiterating, this modelling approach's goal is not to calibrate runoff and sediment yield for this catchment, but to provide a dynamic and spatial distributed evaluation of its hydrologic and erosive fragility for an actual rainfall event. This is, therefore, the reason for the chosen data parametrization for the simulations.

Table 5 – Rainfall events characteristics.

Event (d/m/y)	Precipitation (mm)	Duration time (minutes)	Previous rainfall (48 hours)
08/10/2015	35	84	43.68
19/11/2015	80	222	14.07
14/12/2015	36	522	46.62
29/12/2015	25	168	16.8

Fine sediment fingerprinting – Work pack III

This work pack uses an alternative fingerprinting method based on NIR spectroscopy and SVM modeling, and two sampling strategies for fine sediment source identification. They were divided in Fingerprinting 1 and 2 (FP1 and FP2). FP1 was based on spatial sources, the endmembers being the previously mentioned three headwater sub catchments. This tributary approach will indicate which sub catchment contributes with greater amounts of sediment that reaches GMex.

FP2 considers source types (topsoil, forest, unpaved roads and stream channel) within each sub catchment, aiming to address which land uses or landscape components are contributing more sediment to their outlets. Therefore, sediment samples were both sources and sink on FP1, while on FP2 soil samples were sources and sediment samples, sinks.

Soil and sediment sample collection

Soil source samples (Figure 9) were individually selected based on visual evidence of erosion or soil degradation and connectivity to the drainage network. They include the land uses and landscape components: cropfields, grasslands, stream channels, forests and unpaved roads. Samples from cropfields and grasslands compose the source type topsoil. Samples were collected over each sub catchment. On each location, 5 sub-samples were collected, mixed and homogenized to compose a sample representing the area (Table 6). Samples were collected on the soil surface (0 – 2 cm of depth), due to the likelihood of surface material to be mobilized by water erosion, or where there was evidence of erosion.

Figure 9 – GMex catchment and geological formations, highlighting the three sub catchments and sample location. Red circles represent catchment outlets.

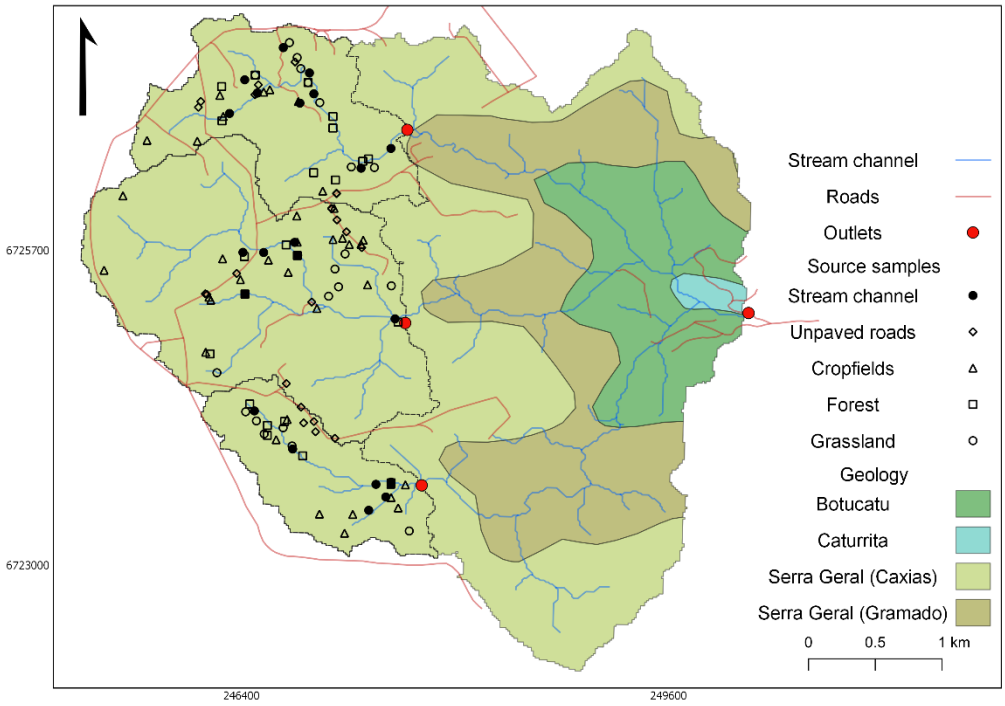

Source: Author.

Regarding the sediment material, deposited bed sediment samples were collected along the water channels at the outlets of S1, S2, S3 and at GMex, between January and June 2019. Sediment samples of each sub catchment are considered drains on FP1. Since

these sub catchments have its channels meet downstream at the GMex, the samples are considered sources on FP2. All four locations can be seen in Figure 9. Care was taken when collecting sediment samples so losses of fine material were reduced.

Table 6 – Number of collected source and sediment samples.

Catchment/ Sources	**Source samples**						**Sediment samples**
	Cropfields	Unpaved Road	Stream Channel	Grassland	Forest	**Total**	Deposited sediment
S1	8	9	9	7	6	39	7
S2	14	9	6	6	6	41	6
S3	6	6	6	6	6	30	6
GMex	-	-	-	-	-	-	6
Total	28	24	21	19	18	**110**	15

All samples were dried in ovens with forced air circulation and temperature between 40 and 50°C. Later, samples were gently disaggregated and sieved for obtaining the granulometric fraction of diameter smaller than 63 µm, so particle size differences were minimized.

Sample and data analysis

In order to calibrate the prediction models and test the analyzed properties' additive behavior, artificial mixtures were made using source's samples. The sample range attempts to account for spectral diversity, and it was also used for calculating the model's confidence statistics by testing its performance. First, samples of each potential source were mixed in equal weight proportions to comprise one reference sample. Then, from these, others were created by mixing different proportions to build the statistical model. For FP1, 37 artificial mixtures were created with the sediment samples from each sub catchment. Their distribution can be visualized in a ternary diagram (Figure 10). While for FP2, 72 artificial mixtures were created covering a range from 0 to 90% of a given source sample (Chart 1 in Appendix A).

For this study, the samples' absorbance was analyzed by near-infrared spectroscopy. The spectra range from 12000 to 4000 cm^{-1} was scanned, using the Bruker

MPA FT-NIR (Fourier transform near-infrared) spectrometer, at a resolution of $2cm^{-1}$. Samples were carefully placed in a Petri dish prior to scanning and background readings were regularly performed.

Data was manipulated using the R environment (R Core Team 2019). The spectra dataset was transformed by a smoothing and data derivative algorithm, Savitzky-Golay derivative, first-order polynomial (11 window points) (Savitzky and Golay 1964). By calculating the first derivative, this pre-processing calculates the change rate between absorbance and wavelength, highlighting peaks. This is available in R package "prospectr" (Stevens and Ramirez-Lopez 2013), which was developed for preprocessing visible and near infrared diffuse reflectance data.

Data from the artificial samples was randomly separated on calibration and validation sets (70 and 30%, respectively). This partitioning was later used for evaluating the models' performances. Statistical indicators coefficient of determination (R^2), root mean square error (RMSE) and mean error (ME) were calculated for comparing calibration and validation datasets of each model.

Then, for establishing a relationship between spectral data (x variable) and the contribution of a given source (y variable), support vector machine models were used. A total of 15 Support Vector Machine (SVM) regression models were independently trained, one for each sediment source, using a linear kernel.

The models were used for predicting the contribution proportion of each potential source to the sediment loads individually. The sum of source contribution ranged between 0 and 100 and closely added up to 100% (Appendix A). Poulenard et al. (2009) attributed the slight variations to the fact that the calibration is made using soil samples, while the prediction is on sediment samples.

Figure 10 – Ternary diagram representation of sample proportions used to compose artificial mixtures for model calibration in Fingerprinting 1.

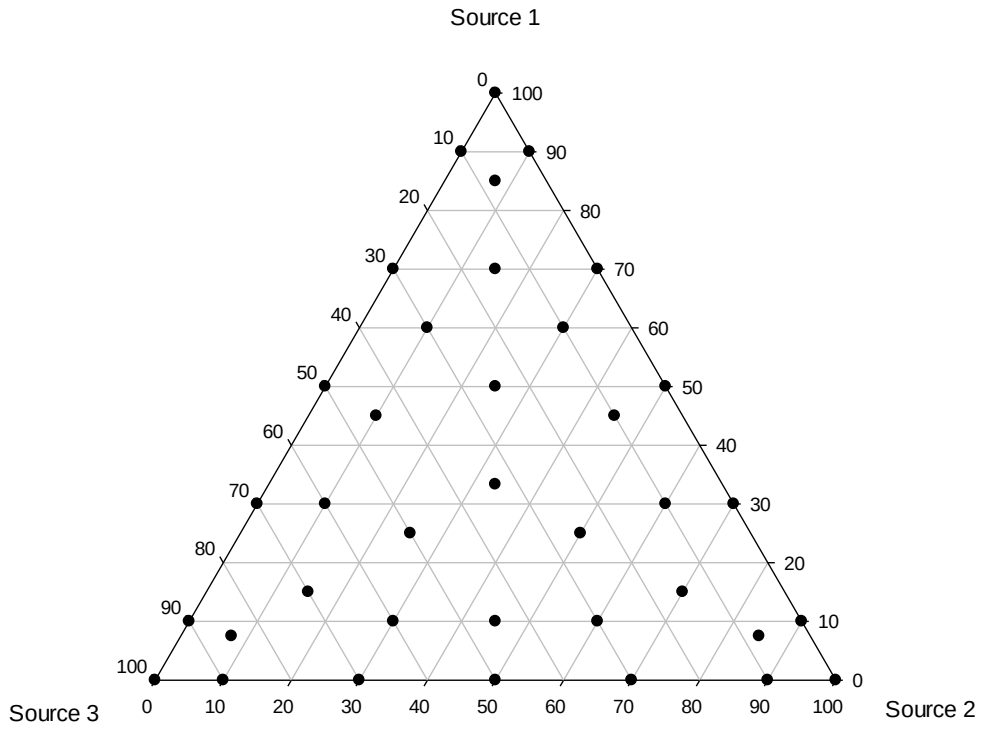

Source: Author.

Results and discussion

Terrain analysis – Work pack I

For addressing the influence of the topographic factor, the results are presented by dividing zones of prospecting erosion susceptibility in different value classes.

The slope range (Figure 20 in Appendix B) varies between these sub catchments. Most areas of S1's area have slopes varying within 0 and 8%, 40% of the area between 8 and 20%, and 15% between 20 and 45% (Figure 11). S2 is the least steep of the sub catchments, around 60% of the area has gentle slopes, from 0 to 8%, and the remaining ranges from 8 to 20% (Figure 11). Flat slopes occupy less than 10% of S3's area and 40% ranges from 3 to 8% (Figure 11). Slopes from 8 to 20% occupy 40% of the area, being this the sub catchment with most area within this range, and less than 10% of the area ranges from 20 to 45% (Figure 11). Steeper slopes are located closer to the streams on S1 and S3. Regarding the drainage area of GMex, slopes from 45 to 75% occur over the transition between the Plateau and Central Depression.

Most of the areas with steeper slopes of these sub catchments are occupied by forests. Dense covers, such as forests, can be responsible for intercepting nearly 25% of precipitation (Julien 2002). This can delay the time for soil infiltration to be exceeded and limit runoff rates.

Figure 11 – Histogram for terrain slope of sub catchments and GMex.

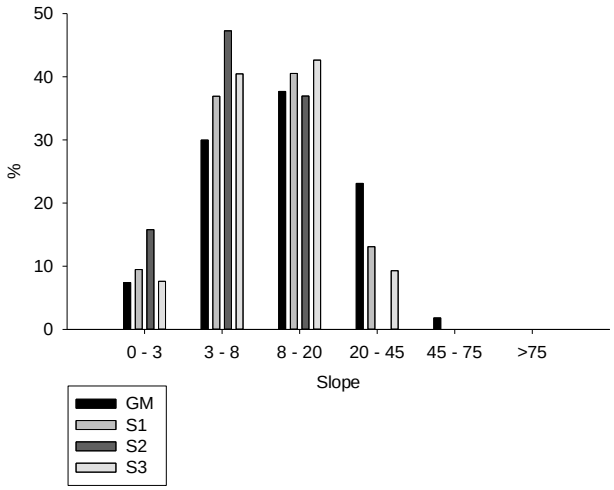

* GM corresponds to the drainage area of Guarda Mor's main monitoring station (GMex).
Source: Author.

Slope shows that S2 tends to have lower punctual erosive capacity than S1 and S3, these catchments show a similar spatial distribution to each other. Erosion analysis by slope alone may not be precisely explanatory, because it is dependent of other factors such as land use and runoff erosive power. However, it is predictable that S1 and S3, besides having a general tendency to increases in flow speed, have higher proportions of shallow soils due to the propensity of soil forming factors, which would implicate in greater amounts of surface runoff.

Nearly 80% of profile curvatures in all sub catchments are flat; and convex and concave surfaces (Figure 21 in Appendix B) correspond each to around 10% of the area. Convex profile curvatures are associated with runoff acceleration and greater susceptibility to soil detachment and sediment transport. Concave ones promote the opposite: a decrease in runoff speed and, eventually, deposition processes. Convex and concave segments are present in very similar proportions in all basins. Therefore, the

susceptibility is enhanced by the land surface propensity to being eroded, such as surfaces that are mobilized and soil that is exposed.

According to these basins land use, cropfields would be the most likely use to have soil being exposed to runoff disaggregation and transport, making those areas, especially in S2 and S3, more susceptible to soil erosion and sediment yield. Regarding plan curvatures, around 37% of the area of each sub catchment is occupied by planar surfaces. The remaining is occupied by convergent and divergent curvatures, with a slight greater area of divergent surfaces on S1 and S2 (additional 6 and 2%, respectively).

TWI ranged from higher than 6 to almost 15 in the sub catchments (Figure 22 in Appendix B). A few larger zones of planar and linear curvature, which coincide with high TWI values, point the presence of zones where runoff and sediment might accumulate. Those usually humid spots may retain sediment and can be responsible for a dysconnectivity or discontinuity in sediment and runoff transfer. All sub catchments present similar distribution on TWI ranges, with the exception for S2. In S1, areas of higher TWI are found in the upper part of the basin, while S3 has significant areas in its second half.

In agreement to the slope results, S2 has larger area of higher TWI values than the other two (Figure 12). The higher TWI is proportional to increased catchment area and smaller slope. This shows this catchment has greater potential for the presence of zones of water accumulation or saturation and therefore sediment retention, which may result in a decrease in sediment connectivity to the stream. Minella and Merten (2012) found these saturated zones to occupy small areas yet the authors highlighted the importance they have on a catchment's hydrological functions and regime, such as decreasing peak discharge and on aquifer recharge.

Figure 12 – Histogram for Topographic Wetness Index (TWI) of sub catchments 1, 2 and 3 and GMex.

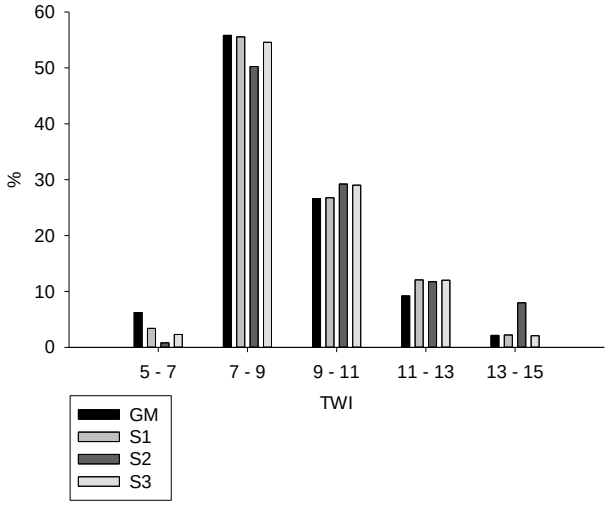

* GM corresponds to the drainage area of Guarda Mor's main monitoring station (GMex).
Source: Author.

Besides these concentrated zones, higher TWI ranges on a hillslope can be associated to a propensity in forming concentrated erosion channels over thalwegs. This can be observed in this catchment's cropfields, by a visual comparison between high TWI and satellite images (Figure 13). The same was observed with the SPI, which is also higher when closer to the drainage network.

Figure 13 – Overlapped images for high values of TWI (top) and SPI (bottom) and satellite images in sub catchment S1.

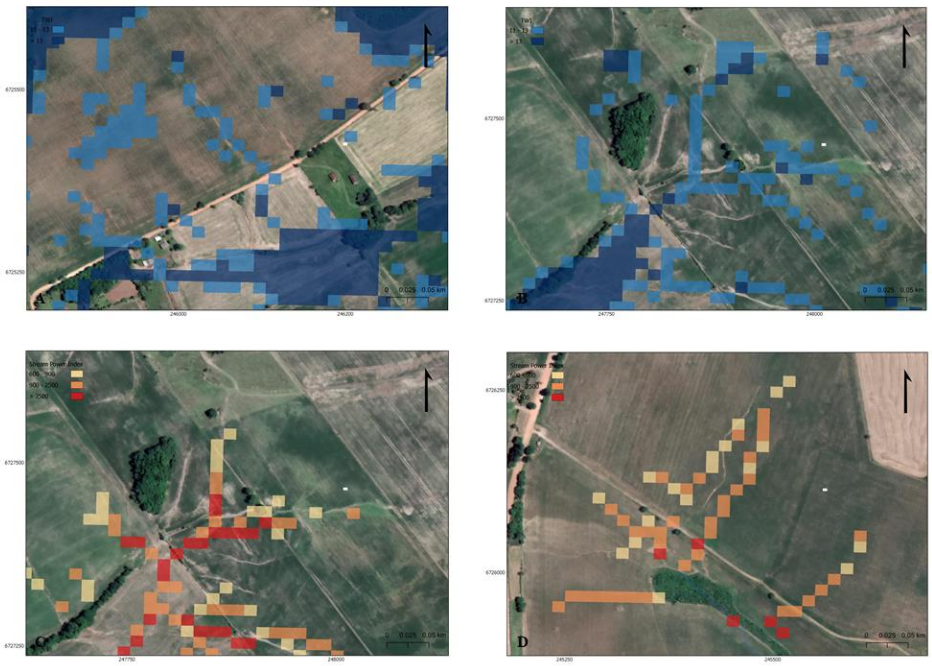

Source: Author.

SPI ranged from 0 to around 19000 in S1, 21000 in S2 and 14000 in S3 (Figures 14 and 23 in Appendix B). In S2, there seems to be small segments of lower SPI values in a disposition which points slightly disconnecting paths. This could be related to poor altimetry resolution (1m) in capturing the relief or indicate some lack of continuity in material transfer within this catchment, corresponding to the previously mentioned zones of higher TWI. Less evidently, this can be observed in the other two catchments.

SPI indicates both flow's volumetric potential, since it uses accumulated catchment area, as its increase in speed, given by slope. It can be seen in Figure 14 that data was separated in seven classes, for each sub catchment and GMex, though only the last reaches values above 25000. The majority of the area has values corresponding to less than 3750. The differences are observed in the remaining area, where S3 appears to show a greater tendency to sediment delivery per area, given its greater percentage of higher SPI values and smaller accumulated area (1.4 km²). S1 has distributed proportions similar to S3. S2 is different of S1 and S3 in this value distribution, indicating a smaller energetic activity of runoff in this area, given its response over hillslopes. However, regarding channel erosion, greater accumulated area would reflect in greater channel erosion in S2, which registered the higher SPI value.

Figure 14 – Histogram for Stream Power Index of sub catchments and GMex.

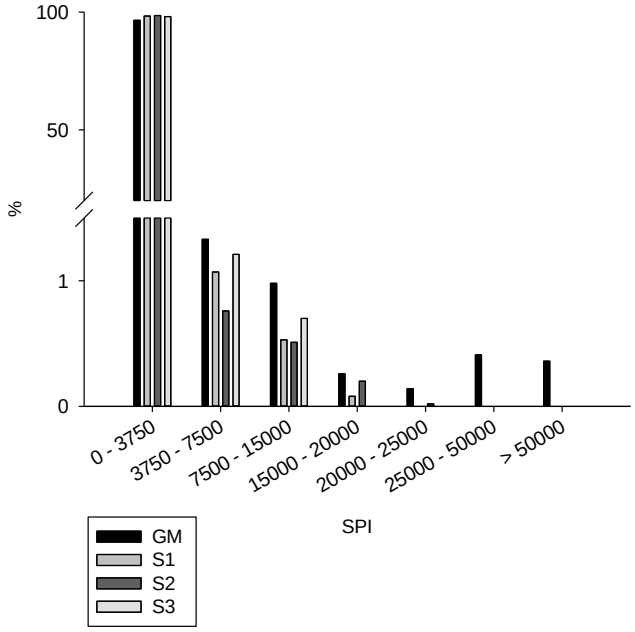

* GM corresponds to the drainage area of Guarda Mor's main monitoring station (GMex).
Source: Author.

LS factor ranged from 0 to 7.76 in S1, 0 to 4.24 in S2 and 0 to 6.74 in S3 (Figure 15). Higher values are also located closer to the drainage network (Figure 24 in Appendix B). In S2, LS factor reached a lower value than the other two catchments, though the discontinuity among its higher values are also more evident. S1 and S3 show high and very condensed areas of higher values combining the steepness and slope length in these zones, showing their potential for erosion and material transport. Since LS Factor considers the same primary attributes as TWI and SPI, their behavior is likewise.

Figure 15 – Histogram for LS Factor of sub catchments and GMex.

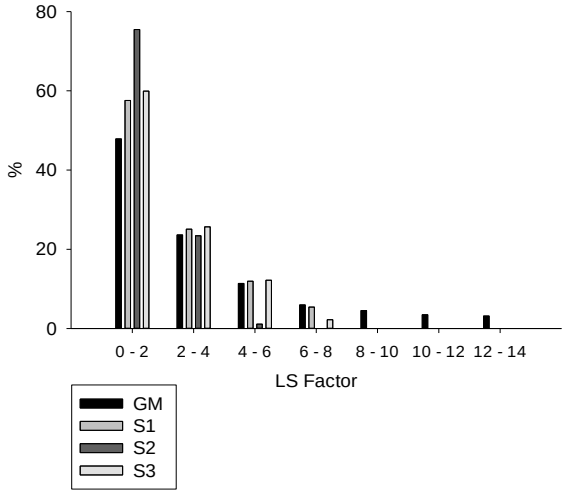

* GM corresponds to the drainage area of Guarda Mor's main monitoring station (GMex).
Source: Author.

With reference to these indexes, Momm et al. (2012) used the TWI to identify the location of ephemeral gullies. Mihret et al. (2018) also found TWI to be successful in predicting gully formation, along with SPI. In addition, Vijith et al. (2019) determined that slope, SPI and the LS factor were some of the most crucial variables in contributing to erosion susceptibility in a catchment. Overall, in these sub catchments, higher values of TWI, SPI and the LS Factor are associated with areas near the drainage network and with forest vegetation. Yet, some of these more fragile zones are currently occupied by cropfields, over convergent landscape zones, and eventually cross with unpaved roads. These two landscape components are prone to runoff generation (Ziegler et al. 2000; Londero et al. 2017), which concentrates and can be led towards forests and riverbanks.

In general, by means of these attributes and indexes, S1 and S3 have a very similar geomorphological arrangement, except for curvatures. In view of relevant indexes for flow accumulation (SPI and LS), S1 and S3 have a higher energetic availability for runoff erosion compared to S2.

Erosion modelling – Work pack II

The spatial distribution of surface runoff and sediment yield remained mostly the same for the different simulated rainfall events. Since only the precipitation volume, rainfall duration and imbibition were altered for each event, these results' visualization

(Figures 25 to 28 in Appendix C) was enhanced by the events of greater volume or magnitude.

Table 7 shows the values for surface runoff, in m³, and sediment yield, in kg, simulated at the outlet of each sub catchment. The amount of m³ of surface runoff observed at the outlet of S2 was always the highest, compared to the other sub catchments. S1 and S3 had, respectively, the overall second highest and lowest amounts of surface runoff at its outlets and for every event. The same pattern is observed when runoff in mm is analyzed, from dividing the volume by the sub catchment's area, as seen in Figure 16. In this analysis, S1 and S3 behave similarly for event 2.

Runoff's spatial distribution shows its connectivity from upper segments of these catchments increases with higher magnitude events. The simulation of event 4 shows that, for this lower volume over a greater period of time, besides showing the lowest values, flow seems to be less connected to the drainage network. For instance, the highest surface runoff volumes are not those observed at the outlet, but upstream of it, representing a slight increase to 101.69, 141.22 and 9.92 m³ in S1, S2 and S3, respectively. Event 2, contrarily, reproduces the event of greater volume and magnitude, and also of visually better flow connectivity.

Table 7 – WATERSED runoff and sediment yield modelling results.

Event	Date (d/m/y)	Sub catchment	Sediment yield (kg)	Surface runoff (m³)
			-modeled values observed at the outlet-	
1	08/10/2015	S1	52.04	494.99
		S2	367.38	1111.63
		S3	6.23	232.48
		GMex	1344.25	6044.70
2	19/11/2015	S1	10004.65	14401.65
		S2	97361.02	36454.46
		S3	20695.29	9640.75
		GMex	48992.80	123517.69
3	14/12/2015	S1	54.19	497.73
		S2	406.72	1114.46
		S3	6.65	251.03
		GMex	263.64	6003.92
4	29/12/2015	S1	15.00	99.15
		S2	52.35	140.15
		S3	2.04	1.78
		GMex	108.39	1619.93

Figure 16 – Histogram for mm of runoff simulated for each sub catchment and GMex.

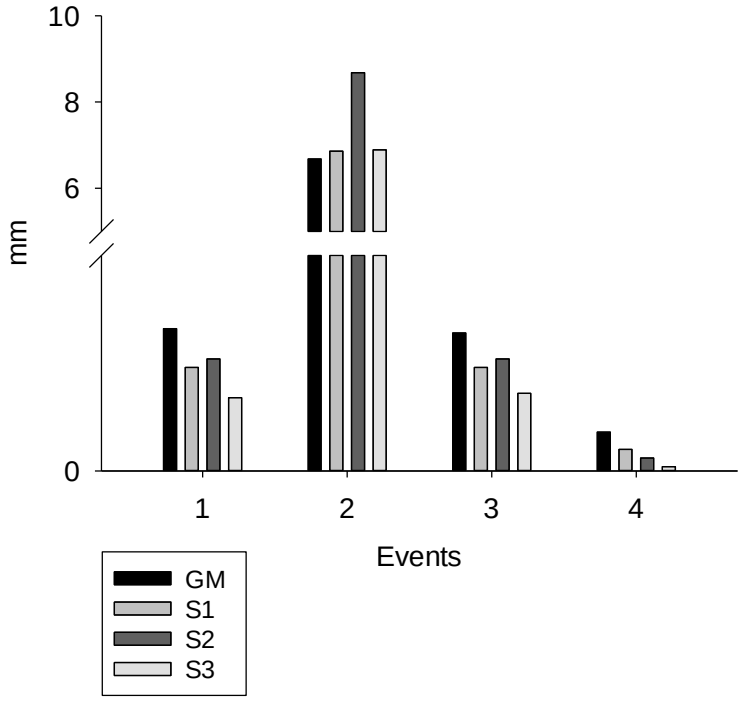

* GM corresponds to the drainage area of Guarda Mor's main monitoring station (GMex).
Source: Author.

Regarding sediment yield, results show a similar pattern, they increase with rainfall volume and are the highest on S2, followed by S1 and S3, on events 1, 3 and 4. The difference regards event 2, in which S1 has the lowest sediment yield. If considering only the obtained simulated values at the outlet of each sub catchment, differently from results indicating similarities between S1 and S3 according to their topographic attributes, greater the fragility of S1 is evidenced by its higher sediment yields. Yet, the highest sediment yield in S3 is not observed at its outlet, reaching 63.64 and 72.63 kg for events 1 and 3, and for event 2, this sub catchment has also the second highest values for sediment yield. This pattern is observed in Figure 17, where the highest sediment yield values were transformed to sediment yield in kg ha^{-1}, only for event 4 this catchment's results are the lowest. Resulting in greater fragility to S3, compared to S1, although less connected. The differences in higher values observed away from the outlet, are possibly due to re-infiltration and sediment deposition calculated by the model.

Figure 17 – Histogram for kg ha^{-1} of sediment yield simulated for each sub catchment and GMex.

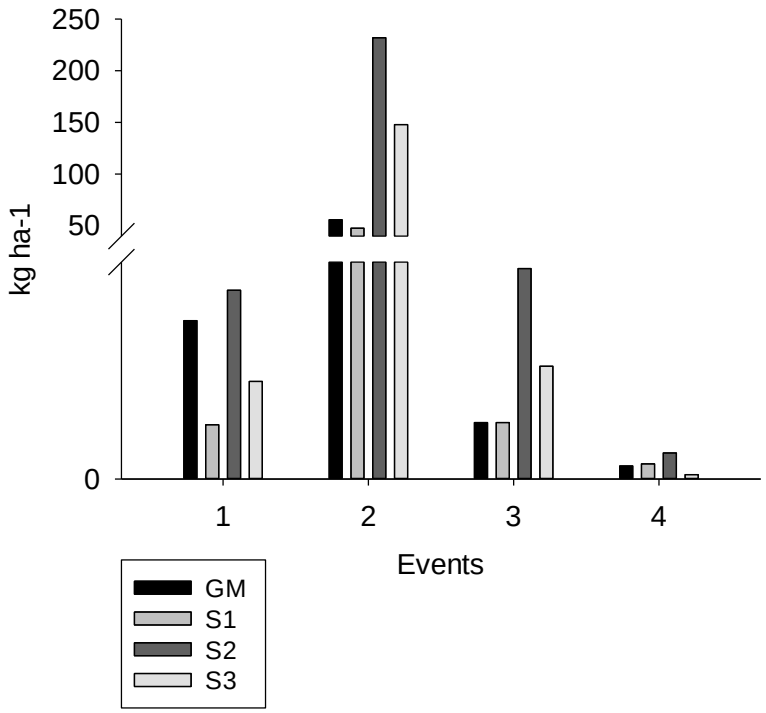

* GM corresponds to the drainage area of Guarda Mor's main monitoring station (GMex).
Source: Author.

With greater catchment area, in general, S2 is the sub catchment with greater potential for runoff and sediment yield. The maps show once more that the most susceptible areas seem to be located near headwater's, near the drainage and steepest areas, in accordance with observations from WP1. They become more evident and pronounced with greater rainfall intensity.

Fine sediment fingerprinting – Work pack III

Calibration results' statistical coefficients show good performance by the models, yet validation results had a large variation, from poor to good results. The plotted results for model calibration and validation for each source can be seen in Appendices D to G. The models for unpaved roads and forest were the best performing ones in every sub catchment, with R^2 for calibration between 0.99 and 1, and for validation between 0.71 and 0.93, indicating their greater discrimination. For all models, the summed predictions reached totals slightly greater than 100%, in line with the overestimation Poulenard et al. (2009) found and attributed to the differences in soil and sediment material used for model calibration and prediction.

The NIR range of soil spectra in influenced by different soil attributes. The spectral range 1100 – 2500 nm responds to total N, organic carbon, specific surface area and water; soil texture also influences spectral behavior (Viscarra Rossel et al. 2006). Therefore, samples from forest may present greater discrepancy from other sources because of higher organic matter, resulting in better distinction and model performance (Brosinsky et al. 2014a), apart from S2. While the lack of organic matter in soils collected on unpaved roads may be responsible for its better discrimination. Tiecher et al. (2015) also found better discrimination of this source in Arvorezinha catchment, using NIR spectra. The authors attributed the results to less organic matter and different clay minerals composition.

This study's models for topsoil have poor R^2 results for model validation, ranging from 0.28 to 0.36. This may be due to spectral overlap from cropfields and grasslands' samples. Verheyen et al. (2014) submitted cropland and grazing land's samples to a PCA analysis prior to establishing source groups. This analysis could not differentiate those two sources in the Vis-NIR spectra range. Then, the authors later created a PLSR model considering all samples of those sources as one group (topsoils). R^2 for that model was 0.947. Although samples from both sources were also considered as one group in this study, R^2 for validation did not improved significantly. Regarding stream channels, Tiecher et al. (2015) associated this source's discrimination to the fact that soils near to the drainage network are subject to biogeochemical alterations due to oxi-reduction reactions, leading to a different mineral composition and, therefore, spectral reading.

For predicted sediment contribution in S1, topsoil, unpaved roads and forest show variations time (Table 8). Stream channels show smallest time variations in percentual contributions. For sample 6 (23/01), 50% of sediment contribution to deposited samples were from unpaved roads. This source averaged 41% contribution, the overall highest contributing source for this catchment. Stream channels showed near constant contributions for the sample's sediments, averaging a 28% contribution. Forest had the smallest contributing percentual. Topsoil in this sub catchment showed the lowest average contribution, cropfields might not have contributed with much sediment as the soil use corresponds to a no-till system in which, as Londero et al. (2017) and Deuschle et al. (2019) results show, biomass maintained over the soil decreases sediment yield from agricultural plots. Although they might show decreased sediment yield, surface runoff may have concentrated and been responsible for greater contributions from other

landscape components downstream from the cropfields and grasslands, such as forests and stream channels.

Table 8 – Percentage of sediment source contribution for samples collected at the outlet of sub catchment 1.

Sediment Sample*	**Sources**				
	Topsoil	Stream Channel	Unpaved Road	Forest	**Total**
1	16.19	25.99	57.48	4.92	104.58
2	29.83	26.19	38.78	9.06	103.86
3	28.89	25.96	37.01	12.48	104.34
4	38.53	28.92	28.84	7.12	103.41
5	25.70	31.64	36.12	11.15	104.61
6	19.86	30.31	50.01	3.68	103.86
Average	**26.50**	**28.17**	**41.37**	**8.07**	**104.11**
R^2 cal	1.00	1.00	1.00	0.99	
R^2 val	0.36	0.37	0.92	0.90	

* Sample number corresponds to collection dates May 1st (1), June 12th (2), July 18th (3), February 22nd (4), March 22nd (5) and January 23rd (6) of 2019.

As seen in Table 9, S2 shows the smallest average forest contribution, except for sample 3 (18/07), which S1 and S3 also had greater contributions from forest for sample 3. This may be related to runoff's flow path, passing through forests prior to reaching the stream channel. Unpaved roads were also the highest sediment contributing source on S2, averaging 50% and reaching near 60% of sediment contribution in sample 1 (01/05). Topsoil used for agriculture contributed with an average 27% in S2. Stream channel contribution varied from near 15 to 38%, averaging 23% of the collected deposited sediment.

Table 9 – Percentage of sediment source contribution for samples collected at the outlet of sub catchment 2.

Sediment Sample*	**Sources**				
	Topsoil	Stream Channel	Unpaved Road	Forest	**Total**
1	28.12	19.43	59.49	-4.65	102.39
2	38.52	14.75	51.25	-2.14	102.38

3	17.60	17.55	51.55	15.77	102.47
4	28.10	28.67	45.93	0.11	102.81
5	32.73	22.08	50.89	-2.90	102.80
6	20.98	37.63	43.37	0.93	102.91
Average	**27.68**	**23.35**	**50.41**	**1.19**	**102.63**
R^2 cal	1.00	1.00	0.99	0.99	
R^2 val	0.32	0.37	0.80	0.29	

* Sample number corresponds to collection dates May 1st (1), June 12th (2), July 18th (3), February 22nd (4), March 22nd (5) and January 23rd (6) of 2019.

In S3 there appeared to be a different dynamic in sediment source contribution (Table 10), accordingly with this catchment's dynamic in work pack II. Unlike the previous sub catchments, the main sediment source for S3 are topsoils (59% average), while unpaved roads are the next greater source. Stream channel has the lowest percentual compared to the other sub-basins, which varied between 5 and 20%. Accordingly, this sub catchment also has forest as the lowest apportionment, less than 7% average.

Lowest contribution from unpaved roads in this sub catchment could be due to fewer road segments within its drainage area, compared to S1 and S2, and their location by the upper segment of the sub catchment (Figure 9). In S1 and S2, roads cross the drainage network twice and have an extension close to 4500 and 5000 meters, respectively. While in S3, their extension is less than 900 meters long and roads do not cross the drainage network.

Table 10 – Percentage of sediment source contribution for samples collected at the outlet of sub catchment 3.

Sediment Sample*	**Sources**				
	Topsoil	Stream Channel	Unpaved Road	Forest	**Total**
1	53.60	17.99	24.08	6.61	102.28
2	61.01	10.08	27.11	5.16	103.36
3	57.32	5.02	28.67	11.30	102.31
4	59.75	9.93	25.32	6.89	101.89
5	62.90	10.17	31.52	-2.45	102.14
6	66.95	5.92	28.63	0.91	102.41
7	51.86	20.39	30.26	-0.07	102.44
Average	**59.06**	**17.99**	**24.08**	**6.61**	**102.40**

R^2 cal	1.00	1.00	1.00	0.99
R^2 val	0.28	0.39	0.93	0.71

* Sample number corresponds to collection dates May 1st (1), August (2), June 12th (3), July 18th (4), February 22nd (5), March 22nd (6) and January 23rd (7) of 2019.

Results show that there is a significantly constant contribution from unpaved roads in all 3 sub catchments (Figure 33 in Appendix H), especially from S2, where the percentual contribution was higher for all samples. Stream channels are also a constant contribution in all catchments, although in smaller values in S3. Differently, in S3 topsoil seem to provide constant and significant sediment contributions.

As for sediment sourcing Guarda Mor tributaries (Table 11 and Figure 33 in Appendix H), results show that, on average, almost 90% of fine sediment is traced back to S1 and a null contribution from S3. S2's contribution varied in time from 10 to 29%. The negative results found for S3 and poor validation statistical results indicate the need for addressing this study with different tracers for more accurate modelling. The results may be associated to the geological differences found downstream from the sub catchment's outlets and unsampled sources. In the future, more points should be sampled for fingerprinting tributaries, such as Habibi et al. (2019) did to increase sample representativeness.

Table 11 – Percentage of sediment source contribution for samples collected at the outlet of GMex.

Sediment Sample*	**Sources**			
	S1	S2	S3	**Total**
1	93.95	29.40	-23.20	100.15
2	84.35	11.46	6.15	101.96
3	84.30	19.59	-3.35	100.54
4	92.43	21.54	-13.42	100.55
5	85.82	10.55	5.16	101.52
Average	**88.17**	**18.50**	**-5.73**	**100.94**
R^2 cal	1.00	1.00	1.00	
R^2 val	0.58	0.93	0.37	

* Sample number corresponds to collection dates May 1st (1), July 18th (2), February 22nd (3), March 22nd (4) and January 23rd (5) of 2019.

Besides, a principal component analysis was performed using the package "Factoshiny" (Vaissie et al. 2020) in R environment (R Core Team, 2019), for the sediment samples used in Fingerprinting 1. Samples from S1, S2 and S3 are located close to each other in the first dimension, in which the percentage of explained variance in the dataset is 87.27%. Yet, samples from S2 separate from S1 and S3 in the second dimension, explaining 9.94% of the variation. The samples from GMex are well separated from the sub catchments' in both first and second dimensions (Figure 18).

Figure 18 – Individuals factor map from Principal Components Analysis for sediment samples for the outlets of sub catchments 1, 2 and 3, and GMex.

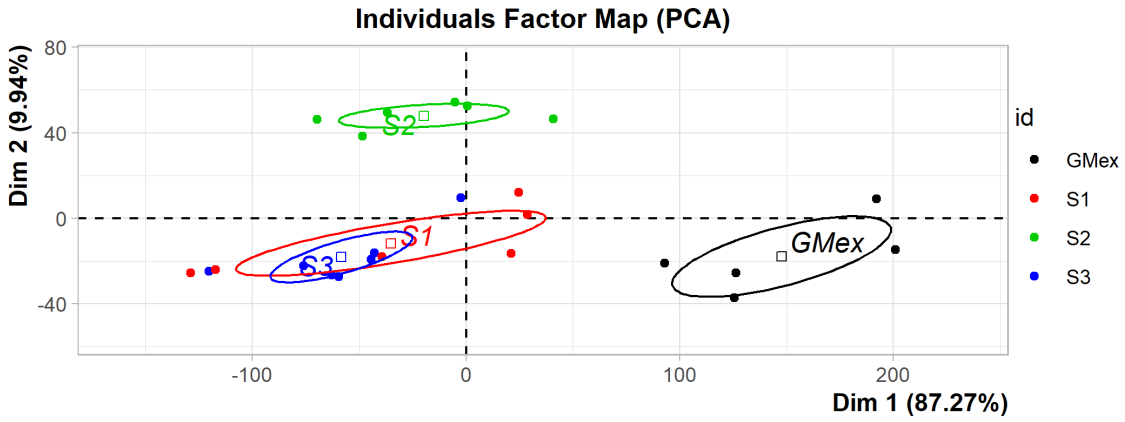

Source: Author.

A hierarchical cluster analysis (Figure 19) separates samples from GMex in a first cluster, while sediment from S1, S2 and S3 are in a second cluster. This shows there is a most significant difference among sediment samples from GMex and upstream catchments. Once again, highlighting the need to address unsampled regions which could be diluting the contribution from the three sub catchments.

Figure 19 – Dendrogram from Hierarchical Cluster Analysis on sediment samples from the outlets of sub catchments 1, 2 and 3, and GMex.

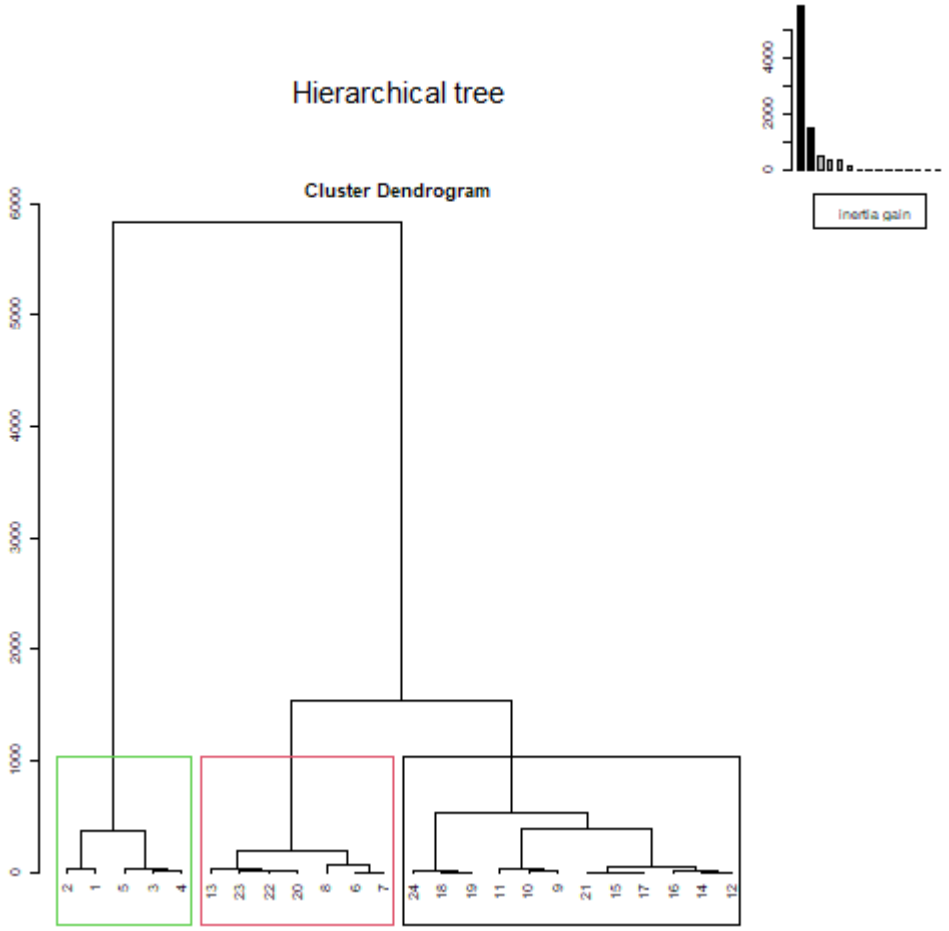

* Samples 1 to 5 were collected at GMex, 6 to 11 at S2, 12 to 18 at S3 and 19 to 24 at S1.
Source: Author.

Integrated observations

Generally, as seen in maps for the hydrological indexes and modelling results, although there is some level of dysconnectivity, or impediment for material or flow transfer between landscape components and to the drainage network, among the sub catchments, in all of them, the areas most fragile to erosion are those near the drainage network, very upstream, spots of greater connectivity. These spots have the potential to accumulate upstream runoff and run-on and are possibly the places with reduced infiltration over the landscape. Where even on lower magnitude rainfall events, as seen in WP2's results, there is a sufficient amount of runoff reaching the lower segments of the hillslopes and, soon after, connecting them to the river channel (Bracken and Croke 2007). Also, hydrological connectivity is most likely to exist where transport the distance from hillslope to channel is shorter (Bracken and Croke 2007). As mentioned before, those spots can also be associated with the formation of rill and gully erosion, which act

as pathways for runoff to concentrate and be delivered with high transport and erosive energy to the drainage network.

Fingerprinting results, such as found by Tiecher et al. (2018) in an agricultural catchment in South Brazil, show high sediment contribution from topsoil and the stream channels. Yet, the topsoil contribution was most relevant in suspended sediment samples (Tiecher et al. 2018), future studies in this catchment should consider samples collected during events. Stream channels' sediment contribution could be due to runoff leaving cropfields and grasslands with great energy to erode riverbanks, and to transport sediment from these sources. This source is not accounted for sediment yield in WP2, making it, along with unpaved roads, difficult to compare results and, therefore, causing uncertainty. Other uncertainties regard the unsampled area between the sub catchments' outlets and of GMex; and the unaddressed in WP1 and WP2 sources, that are important in WP3.

S3 seems to be the sub catchment with the most fragile zones to erosion, according to WP1's results. As for WP2's results, it is the sub catchment with second greatest sediment yield, yet least susceptible to runoff, which would agree with WP3's results for lowest sediment contribution to GMex. At S3, sediment fingerprinting (WP3) shows that the sources with greater contributions come from topsoil. Differently from S1 and S2, where the greatest sediment contribution comes from unpaved roads, a landscape component that is not a natural geomorphological feature addressed by WP1 and WP2. Therefore, for S3, terrain analysis provided a good representation for addressing erosion caused by overland flow over topographically fragile areas.

Terrain analysis shows S1 and S3 to be similar, but they behave differently in WP3's results, where the first has more similarities to S2. On WP2, S2 showed great potential for runoff yielded at the outlet, although it is the one with apparently highest dysconnectivity caused by sinks (WP1), but seemingly only during small magnitude rainfall events (WP2). As of fingerprinting for S1 and S2, contributions from topsoil and stream channels are high, but a great proportion of sediment comes from the landscape component unpaved roads. Results from a sediment budget in a small catchment in South Brazil, where roads occupy little landscape area, point a significant sediment source contribution from them, around 36% (Minella et al. 2014). This landscape component has great potential for negative environmental impacts, such as increased runoff generation (Ziegler et al. 2000) and suspended sediment concentration in rivers (Thomaz et al. 2013). The results point that terrain analysis with the grid resolution used in this study fails to show the fragility caused by unpaved roads.

These methodologies lead to results from basic to higher levels of information, from advanced techniques. They address the different processes, from point observation, to the dynamic response of erosive and hydrological process to a rainfall event and, last, to its integration that results in the sediment yield at a catchment's outlet. Despite they are all modelled, the coherence and complementation of their insights, are indicators that there is a possibility for validating the sediment fingerprinting technique once this modelling is validated by monitored and measured data.

Conclusion

According to terrain analysis and erosion and runoff modeling, the areas adjacent to the drainage network for these sub catchments seem to be the most fragile, especially due to the short distances from source to river, promoting good connectivity for material transfer. These areas appear to expand with greater rainfall intensity. Sub catchments 1 and 3 show similarities in its geomorphology and propensity to runoff formation, while fingerprinting shows a different behavior in sediment contribution, except for forests which have the lowest contribution in all sub catchments. Sub catchments 1 and 2 have prevalent contributions from unpaved roads, followed by similar average contributions from topsoil and stream channels. While, in contrast, topsoil contributes with more than half of the fingerprinted sediment in sub catchment 3, only then followed by unpaved roads and stream channels.

Geomorphology appears to be responsible for the susceptibility to soil erosion in these catchments since the addition of land use and other information in modelling erosion does not cause great alterations to those hotspots' spatial distribution. Yet, spatial distribution, in terms of connectivity and expansion of these areas, seems to be affected by the magnitude of rainfall events. Fingerprinting increased knowledge on these catchment's fragility analysis, as it pointed the importance of unpaved roads on sediment contribution not addressed by work packs 1 and 2.

References

Berry, J. K., Delgado, J. A., Pierce, F. J., & Khosla, R. (2005). Applying spatial analysis for precision conservation across the landscape. *Journal of Soil and Water Conservation, 60*(6), 363-370.

Beven, K. J., & Kirkby, M. J. (1979). A physically based, variable contributing area model of basin hydrology/Un modèle à base physique de zone d'appel variable de l'hydrologie du bassin versant. *Hydrological Sciences Journal*, *24*(1), 43-69.

Boardman, J., Vandaele, K., Evans, R., & Foster, I. D. (2019). Off-site impacts of soil erosion and runoff: Why connectivity is more important than erosion rates. *Soil Use and Management*, *35*(2), 245-256.

Bracken, L. J., & Croke, J. (2007). The concept of hydrological connectivity and its contribution to understanding runoff-dominated geomorphic systems. *Hydrological Processes: An International Journal*, *21*(13), 1749-1763.

Brosinsky, A., Foerster, S., Segl, K., & Kaufmann, H. (2014a). Spectral fingerprinting: sediment source discrimination and contribution modelling of artificial mixtures based on VNIR-SWIR spectral properties. *Journal of soils and sediments*, *14*(12), 1949-1964.

Buitrago, E. J. Y., & Martínez, M. L. J. (2016). Modelos de elevación digital (DEM) para evaluar los riesgos de erosión del suelo: un estudio de caso en Boyacá, Colombia. *Agronomía Colombiana*, *34*(2), 239-29.

Cerdan, O., Le Bissonnais, Y., Couturier, A., & Saby, N. (2002a). Modelling interrill erosion in small cultivated catchments. *Hydrol. Process*, *16*, 3215–3226.

Cerdan, O., Souchère, V., Lecomte, V., Couturier, A., & Le Bissonnais, Y. (2002b). Incorporating soil surface crusting processes in an expert-based runoff model: sealing and transfer by runoff and erosion related to agricultural management. *Catena*, *46*(2-3), 189-205.

Companhia De Pesquisa De Recursos Minerais (2013). Serviço Geológico do Brasil. Mapa Geológico do Estado do Rio Grande do Sul. Escala 1:750.000. < http://www.cprm.gov.br/publique/Geologia/Geologia-Basica/Cartografia-Geologica-Regional-624.html>

Deuschle, D., Minella, J. P. G., Hörbe, T. A. N., Londero, A. L., & Schneider, F. J. A. (2019). Erosion and hydrological response in no-tillage subjected to crop rotation intensification in southern Brazil. *Geoderma*, *340*, 157–163.

Durlo, M. A., & Sutili, F. J. (2014). *Bioengenharia: manejo biotécnico de cursos de água*. Santa Maria: Edição do Autor.

Engman, E. T. (1986). Roughness coefficients for routing surface runoff. *Journal of Irrigation and Drainage Engineering*, *112*(1), 39-53.

Gruber, S., & Peckham, S. (2009). *Land-surface parameters and objects in hydrology*. In: Hengl, T., & Reuter, H. I. (Eds.): Geomorphometry: Concepts, Software, Applications.p. 171-194. Elsevier, Amsterdam.

Habibi, S., Gholami, H., Fathabadi, A., & Jansen, J. D. (2019). Fingerprinting sources of reservoir sediment via two modelling approaches. *Science of the Total Environment*, *663*, 78-96.

IUSS Working Group WRB. (2015). World reference base for soil resources 2014, update 2015: International soil classification system for naming soils and creating legends for soil maps. *World Soil Resources Reports No. 106*, 192.

Jancewicz, K., Migoń, P., & Kasprzak, M. (2019). Connectivity patterns in contrasting types of tableland sandstone relief revealed by Topographic Wetness Index. *Science of The Total Environment, 656*, 1046-1062.

Julien, P. Y. (2002). *River mechanics*. Cambridge University Press.

Landemaine, V. (2016). Érosion des sols et transferts sédimentaires sur les bassins versants de l'Ouest du Bassin de Paris: analyse, quantification et modélisation à l'échelle pluriannuelle. Normandie Universitè: Thèse.

Le Bissonnais, Y., Cerdan, O., Lecomte, V., Benkhadra, H., Souchère, V., & Martin, P. (2005). Variability of soil surface characteristics influencing runoff and interrill erosion. *Catena*, *62*(2-3), 111-124.

Londero, A. L., Minella, J. P. G., Deuschle, D., Schneider, F. J. A., Boeni, M., & Merten, G. H. (2017). Impact of broad-based terraces on water and sediment losses in no-till (paired zero-order) catchments in southern Brazil. *Journal of Soils and Sediments, 18*(3), 1159-1175.

McBratney, A. B., Santos, M. M., & Minasny, B. (2003). On digital soil mapping. *Geoderma*, *117*(1-2), 3-52.

Merritt, W. S., Letcher, R. A., & Jakeman, A. J. (2003). A review of erosion and sediment transport models. *Environmental Modelling & Software*, *18*(8-9), 761-799.

Mhiret, D. A., Dagnew, D. C., Assefa, T. T., Tilahun, S. A., Zaitchik, B. F., & Steenhuis, T. S. (2019). Erosion hotspot identification in the sub-humid Ethiopian highlands. *Ecohydrology & Hydrobiology*, *19*(1), 146-154.

Minella, J. P. G., & Merten, G. H. (2012). Índices topográficos aplicados à modelagem agrícola e ambiental. *Ciência Rural, 42*(9).

Momm, H. G., Bingner, R. L., Wells, R. R., & Wilcox, D. (2012). AGNPS GIS-based tool for watershed-scale identification and mapping of cropland potential ephemeral gullies. *Applied engineering in agriculture*, *28*(1), 17-29.

Moore, I. D., Gessler, G.A., & Peterson, G.A. (1993). Soil attribute prediction using terrain analysis. *Soil Science Society of America Journal, 57*, 443-452.

Moore, I. D, Grayson, R. B., & Ladson, A. R. (1991). Digital Terrain Modelling: a review of hydrological, geomorphological, and biological applications. *Hydrological Processes, 5*, 3-30.

Morgan, R. P. C. (2005). *Soil erosion and conservation* – 3rd ed. Longman: Blackwell.

Poulenard, J., Perrette, Y., Fanget, B., Quetin, P., Trevisan, D., & Dorioz, J. M. (2009). Infrared spectroscopy tracing of sediment sources in a small rural watershed (French Alps). *Science of the Total Environment, 407*, 2808-2819.

QGIS.org (2020). QGIS Geographic Information System. Open Source Geospatial Foundation Project. <http://qgis.org>

R Core Team (2019). R: A language and environment for statistical computing. R Foundation for Statistical Computing, Vienna, Austria. https://www.R-project.org/.

Ross, J. L. S. (1994). Análise empírica da fragilidade dos ambientes naturais e antropizados. *Revista do Departamento de Geografia, 8*, 63-74.

Santos, H. G., Jacomine, P. K. T., Dos Anjos, L. H. C., De Olivieira, V. A., Lumbreras, J. F., Coelho, et al. (2018). *Sistema brasileiro de classificação de solos.* Brasília, DF: EMBRAPA.

Savitzky, A., & Golay, M. J. E. (1964). Smoothing and differentiation of data by simplified least squares procedures. *Anal. Chem., 36*, 1627-1639.

Stevens, A., & Ramirez-Lopez, L. (2013). An introduction to the prospectr package. R package Vignette R package version 0.1.3.

Thomaz, E. L., Vestena, L. R., & Ramos Scharrón, C. E. (2014). The effects of unpaved roads on suspended sediment concentration at varying spatial scales–a case study from Southern Brazil. *Water and environment journal, 28*(4), 547-555.

Tiecher, T., Caner, L., Minella, J. P. G., Bender, M. A., & Santos, D. R. (2016). Tracing sediment sources in a subtropical rural catchment of southern Brazil by using geochemical tracers and near-infrared spectroscopy. *Soil & Tillage Research, 156*, 478-491.

Tiecher, T., Caner, L., Minella, J. P. G., & Santos, D. R. (2015). Combining visible-based-color parameters and geochemical tracers to improve sediment source discrimination and apportionment. *Science of the Total Environment. 527*, 135-149.

Tiecher, T., Minella, J. P. G., Evrard, O., Caner, L., Merten, G.H., Capoane, V., Didoné, E. J., & Santos, D. R. (2018). Fingerprinting sediment sources in a large agricultural catchment under no-tillage in Southern Brazil (Conceição River). *Land Degradation & Development, 29*(4), 939-951.

Vaissie, P., Monge, A., & Husson, F. (2020). Perform Factorial Analysis from 'FactoMineR' with a Shiny Application. Package 'Factoshiny' version 2.2.

Verheyen, D., Diels, J., Kissi, E., & Poesen, J. (2014). The use of visible and near-infrared reflectance measurements for identifying the source of suspended sediment in rivers and comparison with geochemical fingerprinting. *Journal of soils and sediments*, *14*(11), 1869-1885.

Vijith, H., & Dodge-Wan, D. (2019). Modelling terrain erosion susceptibility of logged and regenerated forested region in northern Borneo through the Analytical Hierarchy Process (AHP) and GIS techniques. *Geoenvironmental Disasters*, *6*(1), 8.

Viscarra Rossel, R. A., Walvoort, D. J. J., Mcbratney, A. B., Janik, L. J., & Skjemstad, J. O. (2006). Visible, near infrared, mid infrared or combined diffuse reflectance spectroscopy for simultaneous assessment of various soil properties. *Geoderma*, *131*(1-2), 59-75.

Walling, D. E. (2013). The evolution of sediment source fingerprinting investigations in fluvial systems. *J Soils Sediments*, *13*, 1658-1675.

Wohl, E., Brierley, G., Cadol, D., Coulthard, T. J., Covino, T., Fryirs, K. A., et al. (2019). Connectivity as an emergent property of geomorphic systems. *Earth Surface Processes and Landforms*, *44*(1), 4-26.

Yang, Y., Gao, B., Hao, H., Zhou, H., & Lu, J. (2017). Nitrogen and phosphorus in sediments in China: a national-scale assessment and review. *Science of the Total Environment*, *576*, 840-849.

Zevenbergen, L. W., & Thorne, C. R. (1987). Quantitative analysis of land surface topography. *Earth surface processes and landforms*, *12*(1), 47-56.

Ziegler, A. D., Sutherland, R. A., & Giambelluca, T. W. (2000). Runoff generation and sediment production on unpaved roads, footpaths and agricultural land surfaces in northern Thailand. *Earth Surface Processes and Landforms: The Journal of the British Geomorphological Research Group*, *25*(5), 519-534.

5 CONCLUSION

The combination of applied analyses provided different results, yet complementary insights. Terrain analysis and erosion modelling point the fragility of areas near the drainage network and their connectivity, representing possible material transfer. Geomorphological similarities between sub catchments 1 and 3 did not lead to similar sediment contributions. Topsoil, stream channels and unpaved roads are important sediment sources, while forests did not show significant contribution. The obtained information should be of usefulness to public managers.

This methodology is effective in evidencing the fragility of areas where overland flow can concentrate and lead to processes of soil degradation. Although, it fails to show the effect of the landscape component unpaved roads. More detailed terrain representation may overcome this issue. Furthermore, confrontation for fingerprinting results are needed and further analysis, especially fingerprinting sediment from tributaries.

6 REFERENCES

BAGNOLD, R. A. **An approach to the sediment transport problem from general physics.** US government printing office. 1966.

BAIGORRIA, G. A.; ROMERO, C. C. Assessment of erosion hotspots in a watershed: Integrating the WEPP model and GIS in a case study in the Peruvian Andes. **Environmental Modelling and Software**, v. 22, n. 8, p. 1175-1183, 2007.

BARROS, C. A. P.; MINELLA, J. P. G.; DALBIANCO, L.; RAMON, R. Description of hydrological and erosion processes determined by applying the LISEM model in a rural catchment in southern Brazil. **Journal of soils and sediments**, v. 14, n. 7, p. 1298-1310, 2014.

BENAVIDEZ, R.; JACKSON, B.; MAXWELL, D.; NORTON, K. A review of the (Revised) Universal Soil Loss Equation ((R) USLE): with a view to increasing its global applicability and improving soil loss estimates. **Hydrology and Earth System Sciences**, v. 22, n. 11, p. 6059-6086, 2018.

BERRY, J. K.; DELGADO, J. A.; KHOSLA, R.; PIERCE, F. J. Precision conservation for environmental sustainability. **Journal of Soil and Water Conservation**, v. 58, n. 6, p. 332-339, 2003.

BOUDREAULT, M.; KOITER, A. J.; LOBB, D. A.; LIU, K.; BENOY, G.; OWENS, P. N.; DANIELESCU, S.; LI, S. Using colour shape and radionuclide fingerprints to identify sources of sediment in an agricultural watershed in Atlantic Canada. **Canadian Water Resources Journal**, v. 43, n. 3, p. 347-365, 2018.

BROSINSKY, A.; FOERSTER, S.; SEGL, K.; LÓPEZ-TARAZÓN, J. A.; PIQUÉ, G.; BRONSTERT, A. Spectral fingerprinting: characterizing suspended sediment sources by the use of VNIR-SWIR spectral information. **J Soils Sediments**, v. 14, n. 12, p. 1965-1981, 2014b.

CABRAL, J. B. P.; ROCHA, I. R.; MARTINS, A. P.; ASSUNÇÃO, H. F.; BECEGATO, V. A. Mapeamento da fragilidade ambiental da bacia hidrográfica do Rio Doce (GO), utilizando técnicas de geoprocessamento. **GeoFocus** (Artículos), n 11, p. 51-69, 2011.

CAPOANE, V.; SANTOS, L. J. C.; DOS SANTOS, D. R.; TIECHER, T. Uso de atributos topográficos para predição de áreas propensas a perda e a deposição de sedimento em uma bacia hidrográfica do planalto do Rio Grande do Sul. **Revista Brasileira de Geomorfologia**, v. 16, n. 3, 2015.

CAREY, W. P. **Physical basis and potential estimation techniques for soil erosion parameters in the Precipitation-Runoff Modeling System (PRMS)**. US Geological Survey. Vol. 84, N. 4218. 1984.

CHANG, T. J.; BAYES, T. D. Development of erosion hotspots for a watershed. **Journal of irrigation and drainage engineering**, v. 139, n. 12, p. 1011-1017, 2013.

COCHRANE, T. A.; FLANAGAN, D. C. Assessing water erosion in small watersheds using WEPP with GIS and digital elevation models. **Journal of soil and water conservation**, v. 54, n. 4, p. 678-685, 1999.

COLLINS, A. L.; WALLING, D. E. Documenting catchment suspended sediment sources: problems, approaches and prospects. **Progress in Physical Geography**, v. 28, n. 2, p. 159-196, 2004.

COLLINS, A.; WALLING, D.; LEEKS, G. J. L. Composite fingerprinting of the spatial source of fluvial suspended sediment: a case study of the Exe and Severn River basins, United Kingdom. **Géomorphologie: relief, processus, environnement**, v. 2, n. 2, p. 41-53, 1996.

COLLINS, A. L.; WALLING, D. E. Selecting fingerprint properties for discriminating potential suspended sediment sources in river basins. **Journal of hydrology**, v. 261, n. 1-4, p. 218-244, 2002.

DELMAS, M.; PAK, L. T.; CERDAN, O.; SOUCHÈRE, V.; LE BISSONNAIS, Y.; COUTURIER, A.; SOREL, L. Erosion and sediment budget across scale: A case study in a catchment of the European loess belt. **Journal of Hydrology**, 420, p. 255-263, 2012.

DE ROO, A. P. J.; JETTEN, V. G. Calibrating and validating the LISEM model for two data sets from the Netherlands and South Africa. **Catena**, v. 37, n. 3-4, p. 477-493, 1999.

DIDSZUN, J.; UHLENBROOK, S. Scaling of dominant runoff generation processes: Nested catchments approach using multiple tracers. **Water Resources Research**, v. 44, n. 2, 2008.

DUVERT, C.; GRATIOT, N.; EVRARD, O.; NAVRATIL, O.; NÉMERY, J.; PRAT, C.; ESTEVES, M. Drivers of erosion and suspended sediment transport in three headwater catchments of the Mexican Central Highlands. **Geomorphology**, v. 123, n. 3-4, p. 243-256, 2010.

EVRARD, O.; CERDAN, O.; VAN WESEMAEL, B.; CHAUVET, M.; LE BISSONNAIS, Y.; RACLOT, D.; VANDAELE, K.; ANDRIEUX, P.; BIELDERS, C. Reliability of an expert-based runoff and erosion model: application of STREAM to different environments. **Catena**, v. 78, n. 2, p. 129-141, 2009.

EVRARD, O.; DURAND, R.; FOUCHER, A.; TIECHER, T.; SELLIER, V.; ONDA, Y.; LEFEVRE, I.; CERDAN, O.; LACEBY, J.P. Using spectrocolourimetry to trace sediment source dynamics in coastal catchments draining the main Fukushima radioactive pollution plume (2011–2017). **Journal of Soils and Sediments**, v. 19, n. 9, p. 3290-3301, 2019.

EVRARD, O.; NAVRATIL, O.; AYRAULT, S.; AHMADI, M.; NÉMERY, J.; LEGOUT, C.; LEFÈVRE, I.; POIREL, A.; BONTÉ, P.; ESTEVES, M. Combining suspended sediment monitoring and fingerprinting to determine the spatial origin of fine sediment in a mountainous river catchment. **Earth Surface Processes and Landforms**, v. 36, n. 8, p. 1072-1089, 2011.

EVRARD, O.; POULENARD, J.; NÉMERY, J.; AYRAULT, S.; GRATIOT, N.; DUVERT, C.; PRAT, C.; LEFÈVRE, I.; BONTÉ, P.; ESTEVES, M. Tracing sediment sources in a tropical highland catchment of central Mexico by using conventional and alternative fingerprinting methods. **Hydrological Processes**, v. 27, n. 6, p. 911-922, 2013.

FLANAGAN, D. C.; NEARING, M. A. **USDA Water Erosion Prediction Project: Hillslope Profile and Watershed Model Documentation**. NSERL Report No. 10, USDA-ARS National Soil Erosion Research Laboratory, West Lafayette, IN 47907-1194. 1995.

FOSTER, G. R.; MEYER, L. D. **A Closed-Form Soil Erosion Equation for Upland Areas** In: SHEN, H. W., Ed., Proceeding of Sedimentation Symposium to Honor Prof. H. A. Einstein, Vol. 12, Colorado State University, Fort Collins, 1-19. 1972.

GENTINE, P.; TROY, T. J.; LINTNER, B. R.; FINDELL, K. L. Scaling in surface hydrology: Progress and challenges. **Journal of Contemporary Water research & education**, v. 147, n. 1, p. 28-40, 2012.

GOLOSOV, V.; WALLING, D. E. **Erosion and sediment problems: Global issues and hotspots**. Scientific and Cultural Organization: United Nations Educational. 2019.

GOVERS, G. **Misapplications and Misconceptions of Erosion Models. In: Handbook of Erosion Modelling**, 1st edition. Edited by MORGAN, R. P. C. & NEARING, M. A. Blackwell Publishing Ltd. 2011.

HADDADCHI, A.; RYDER, D. S.; EVRARD, O.; OLLEY, J. Sediment fingerprinting in fluvial systems: review of tracers, sediment sources and mixing models. **International Journal of Sediment Research**, v. 28, n. 4, p. 560-578, 2013.

HEINE, R. A.; LANT, C. L.; SENGUPTA, R. R. Development and comparison of approaches for automated mapping of stream channel networks. **Annals of the Association of American Geographers**, v. 94, n. 3, 477-490, 2004.

HUANG, C.; GASCUEL-ODOUX, C.; CROS-CAYOT, S. Hillslope topographic and hydrologic effects on overland flow and erosion. **Catena**, v. 46, n. 2-3, p. 177-188, 2002.

HUON, S.; EVRARD, O.; GOURDIN, E.; LEFÈVRE, I.; BARIAC, T.; REYSS, J. L.; DES TUREAUX, T. H.; SENGTAHEUANGHOUNG, O.; AYRAULT, S.; RIBOLZI, O. Suspended sediment source and propagation during monsoon events across nested sub-catchments with contrasted land uses in Laos. **Journal of Hydrology: Regional Studies**, v. 9, p. 69-84, 2017.

JOERGENSEN, S. E.; FATH, B. D. **Fundamentals of Ecological Modelling: Applications in Environmental Management and Research**. Amsterdam: Elsevier. 2011.

JULIEN, P. Y. **Erosion and sedimentation**. Cambridge University Press. 1995.

KARATZOGLOU, A.; MEYER, D.; HORNIK, K. Support vector machines in R. **Journal of statistical software**, v. 15, n. 9, p. 1-28, 2006.

KAWAKUBO, F. S.; MORATO, R. G.; CAMPOS, K. C.; LUCHIARI, A.; ROSS, J. L. S. **Caracterização empírica da fragilidade ambiental utilizando geoprocessamento**. Anais XII Simpósio Brasileiro de Sensoriamento Remoto, Goiânia, Brasil, p. 16-21, 2005.

KITCH, J. L.; PHILLIPS, J.; PEUKERT, S.; TAYLOR, A.; BLAKE, W. H. Understanding the geomorphic consequences of enhanced overland flow in mixed agricultural systems: sediment fingerprinting demonstrates the need for integrated upstream and downstream thinking. **Journal of Soils and Sediments**, v. 19, n. 9, p. 3319-3331, 2019.

LEGOUT, C.; POULENARD, J.; NEMERY, J.; NAVRATIL, O.; GRANGEON, T.; EVRARD, O.; ESTEVES, M. Quantifying suspended sediment sources during runoff events in headwater catchments using spectrocolorimetry. **Journal of Soils and Sediments**, v. 13, n.8, p. 1478-1492, 2013.

LEMMA, H.; FRANKL, A.; GRIENSVEN, A.; POESEN, J.; ADGO, E.; NYSSEN, J. Identifying erosion hotspots in Lake Tana Basin from a multisite Soil and Water Assessment Tool validation: Opportunity for land managers. **Land Degrad. Dev**, v. 30, p. 1449–1467, 2019.

LENCHA, B. K.; MOGES, A. Identification of soil erosion hotspots in Jimma zone (Ethiopia) using GIS based approach. **Ethiopian journal of environmental studies and management**, v. 8, n. 2, p. 926-938, 2015.

LEPSCH, I. F. **Formação e conservação dos solos**. São Paulo: Oficina de Textos, 2002.

LUCÀ, F.; CONFORTI, M.; CASTRIGNANÒ, A.; MATTEUCCI, G.; BUTTAFUOCO, G. Effect of calibration set size on prediction at local scale of soil carbon by Vis-NIR spectroscopy. **Geoderma**, v. 288, p. 175-183, 2017.

MAESTRINI, B.; BASSO, B. Drivers of within-field spatial and temporal variability of crop yield across the US Midwest. **Scientific reports**, v. 8, n. 1, p. 1-9, 2018.

MARTÍNEZ-CARRERAS, N.; KREIN, A.; GALLART, F.; IFFLY, J. F.; PFISTER, L.; HOFFMANN, L.; OWENS, P. N. Assessment of different colour parameters for discriminating potential suspended sediment sources and provenance: a multi-scale study in Luxembourg. **Geomorphology**, v. 118, n. 1-2, p. 118-129, 2010a.

MARTÍNEZ-CARRERAS, N.; KREIN, A.; UDELHOVEN, T.; GALLART, F.; IFFLY, J. F.; HOFFMANN, L.; PFISTER, L.; WALLING, D. E. A rapid spectral-reflectance-based fingerprinting approach for documenting suspended sediment sources during storm runoff events. **J. Soils Sediments**, v. 10, p. 400–413, 2010b.

MARTÍNEZ-CARRERAS, N.; UDELHOVEN, T.; KREIN, A.; GALLART, F.; IFFLY, J. F.; ZIEBEL, J.; HOFFMANN, L.; PFISTER, L.; WALLING, D.E. The use of sediment colour measured by diffuse reflectance spectrometry to determine sediment sources: application to the Attert River catchment (Luxembourg). **Journal of Hydrology**, v. 382, n. 1-4, p. 49-63, 2010c.

MCINTYRE, D.S. Soil splash and the formation of surface crusts by raindrop impact. **Soil Sci**., v. 85, p. 261-26, 1958.

MINELLA, J. P. G.; MERTEN, G. H. Monitoramento de bacias hidrográficas para identificar fontes de sedimentos em suspensão. **Ciência Rural**, v. 41, n. 3, p. 424-432, 2011.

MINELLA, J. P. G.; MERTEN, G. H.; REICHERT, J. M.; CASSOL, E. A. **Processos e modelagem da erosão: da parcela à bacia hidrográfica**. In: PRADO, R. B.; TURETTA, A. P. D.; ANDRADE, A. G. (Org.). Manejo e conservação do solo e da água no contexto das mudanças climáticas. Rio de Janeiro: EMBRAPA, p. 105-121, 2010.

MINELLA, J. P.; WALLING, D. E.; MERTEN, G. H. Establishing a sediment budget for a small agricultural catchment in southern Brazil, to support the development of effective sediment management strategies. **Journal of Hydrology**, v. 519, p. 2189-2201, 2014.

MOORE, I. D.; BURCH, G. J.; MACKENZIE, D. H. Topographic effects on the distribution of surface soil water and the location of ephemeral gullies. **Transactions of the ASAE**, v. 31, n. 4, p. 1098-1107, 1988.

MOORE, I. D.; BURCH, G. J. Modelling erosion and deposition: topographic effects. **Transactions of the ASAE**, v. 29, n. 6, p. 1624-1630, 1986a.

MOORE, I. D.; BURCH, G. J. Physical basis of the length-slope factor in the universal soil loss equation 1. **Soil Science Society of America Journal**, v. 50, n. 5, p. 1294-1298, 1986b.

MOORE, I. D.; BURCH, G. J. Sediment transport capacity of sheet and rill flow: application of unit stream power theory. **Water Resources Research**, v. 22, n. 8, p. 1350-1360, 1986c.

NEARING, M. A.; JETTEN, V.; BAFFAUT, C.; CERDAN, O.; COUTURIER, A.; HERNANDEZ, M.; LE BISSONNAIS, Y.; NICHOLS, M. H.; NUNES, J. P.; RENSCHLER, C. S.; SOUCHÈRE, V. Modeling response of soil erosion and runoff to changes in precipitation and cover. **Catena**, v. 61, n. 2-3, p. 131-154, 2005.

PALAZÓN, L.; LATORRE, B.; GASPAR, L.; BLAKE, W. H.; SMITH, H. G.; NAVAS, A. Combining catchment modelling and sediment fingerprinting to assess sediment dynamics in a Spanish Pyrenean river system. **Science of the Total Environment**, v. 569, p. 1136-1148, 2016.

PEART, M. R.; WALLING, D. E. **Fingerprinting sediment source: the example of a drainage basin in Devon, UK**. In Drainage basin sediment delivery: proceedings of a symposium held in Albuquerque, NM., 4-8, 1986.

PIMENTEL, D.; HARVEY, C.; RESOSUDARMO, P.; SINCLAIR, K.; KURZ, D.; MCNAIR, M.; CRIST, S.; SHPRITZ, L.; FITTON, L.; SAFFOURI, R.; BLAIR, R. Environmental and economic costs of soil erosion and conservation benefits. **Science**, v. 267, p. 1117-1123, 1995.

POESEN, J.; NACHTERGAELE, J.; VERSTRAETEN, G.; VALENTIN, C. Gully erosion and environmental change: importance and research needs. **Catena**, v. 50, n. 2-4, p. 91-133, 2003.

POULENARD, J.; LEGOUT, C.; NEMERY, J.; BRAMORSKI, J.; NAVRATIL, O.; DOUCHIN, A.; FANGET, B.; PERRETTE, Y.; EVRARD, O.; ESTEVES, M. Tracing sediment sources during floods using Diffuse Reflectance Infrared Fourier Transform Spectrometry (DRIFTS): A case study in a highly erosive mountainous catchment (Southern French Alps). **Journal of Hydrology**, v. 414, p. 452-462, 2012.

QUINN, P. F.; BEVEN, K. J.; LAMB, R. The in (a/tan/β) index: How to calculate it and how to use it within the topmodel framework. **Hydrological processes**, v. 9, n. 2, p. 161-182, 1995.

ROBERTSON, P. G.; BURGER JR., L. W.; KLING, C. L.; LOWRANCE, R.; MULLA, D. V. **New approaches to environmental management research at landscape and watershed scales**. In: Managing agricultural landscapes for environmental quality: strengthening the science base. Eds. Schnepf, M. & Cox, C. 27–50. Ankeny, IA: Soil and Water Conservation Society. 2007.

SANTOS, C. A.; SOBREIRA, F. G. Análise da fragilidade e vulnerabilidade natural dos terrenos aos processos erosivos como base para o ordenamento territorial: o caso das bacias do Córrego Carioca, Córrego do Bação e Ribeirão Carioca na região do Alto Rio das Velhas – MG. **Revista Brasileira de Geomorfologia**, v. 9, n. 1, p. 65-73, 2008.

SCHOLKOPF, B.; SMOLA, A. J. **Learning with kernels: support vector machines, regularization, optimization, and beyond**. MIT press. 2001.

SIMONNEAUX, V.; CHEGGOUR, A.; DESCHAMPS, C.; MOUILLOT, F.; CERDAN, O.; LE BISSONNAIS, Y. Land use and climate change effects on soil erosion in a semi-arid mountainous watershed (High Atlas, Morocco). **Journal of Arid Environments**, v. 122, p. 64-75, 2015.

SINGH, V. P.; WOOLHISER, D. A. Mathematical modeling of watershed hydrology. **Journal of hydrologic engineering**, v. 7, n. 4, p. 270-292, 2002.

TAMENE, L.; ADIMASSU, Z.; ELLISON, J.; YAEKOB, T.; WOLDEAREGAY, K.; MEKONNEN, K.; THORNE, P.; LE, Q.B. Mapping soil erosion hotspots and assessing the potential impacts of land management practices in the highlands of Ethiopia. **Geomorphology**, v. 292, p. 153-163, 2017.

TIECHER, T.; CANER, L.; MINELLA, J. P. G.; EVRARD, O.; MONDAMERT, L.; LABANOWSKI, J.; RHEINHEIMER, D. Tracing sediment sources using mid-infrared spectroscopy in Arvorezinha catchment, Southern Brazil. **Land Degrad. Develop**, v. 28, p. 1603-1614, 2017.

TROMBETA, L. R.; SOARES, F. B.; GONÇALVES, V. S. Fragilidade potencial para processos erosivos da bacia hidrográfica do Córrego do Cedro. **GeoAtos**. Departamento de Geografia da FCT/UNESP, Presidente Prudente, v. 1, n. 12, p. 119-132, 2012.

VISCARRA ROSSEL, R. A.; BEHRENS, T. Using data mining to model and interpret soil diffuse reflectance spectra. **Geoderma**, v. 158, n. 1-2, p. 46-54, 2010.

WALLING, D. E.; OWENS, P. N.; LEEKS, G. J. L. Fingerprinting suspended sediment sources in the catchment of the River Ouse, Yorkshire, UK. **Hydrological Processes**, v. 12, p. 955-975, 1999.

WALLING, D. E. Tracing suspended sediment sources in catchments and river systems. **Science of the Total Environment**, v. 344, p. 159-184, 2005.

WALLING, D. E.; WOODWARD, J. C. Tracing sources of suspended sediment in river basins: a case study of the River Culm, Devon, UK. **Marine and Freshwater Research**, v. 46, p. 327-336, 1995.

WILSON, J. P.; GALLANT, J. C. EROS: A grid-based program for estimating spatially-distributed erosion indices. **Computers & Geosciences**, v. 22, n. 7, p. 707-712, 1996.

WILSON, J. P.; GALLANT, J. C. Digital terrain analysis. **Terrain analysis: Principles and applications**, v. 6, n. 12, p. 1-27, 2000.

WISCHMEIER, W. H.; SMITH, D. D. **Predicting rainfall erosion losses**. Agriculture Handbook, n. 537, Agriculture Research Service, US Department of Agriculture, Washington, DC. 1978.

WOLD, S.; SJÖSTRÖM, M.; ERIKSSON, L. PLS-regression: a basic tool of chemometrics. **Chemometrics and intelligent laboratory systems**, v. 58, n. 2, p. 109-130, 2001.

YANG, C. T. Unit stream power and sediment transport. **J. Hydr. Div.**, ASCE. 1972.

APPENDIX A

Chart 12 – Sample proportions used to compose artificial mixtures for model calibration in Fingerprinting 2.

(continues)

Artificial mixture	Cropfields	Grasslands	Stream channels	Unpaved roads	Forest
1	20	20	20	20	20
2	96	0	2	2	0
3	0	96	2	2	0
4	0	0	96	2	2
5	2	2	0	96	0
6	2	0	2	0	96
7	90	3	3	3	3
8	3	90	3	3	3
9	3	3	90	3	3
10	3	3	3	90	3
11	3	3	3	3	90
12	80	0	0	15	5
13	0	80	15	5	0
14	15	0	80	5	0
15	15	5	0	80	0
16	5	0	0	15	80
17	85	0	5	5	5
18	5	85	5	5	0
19	5	5	85	0	5
20	5	5	0	85	5
21	0	5	5	5	85
22	76	6	6	6	6
23	6	76	6	6	6
24	6	6	76	6	6
25	6	6	6	76	6
26	6	6	6	6	76
27	70	0	10	10	10
28	10	70	10	10	0
29	10	10	70	0	10
30	0	10	10	70	10
31	10	10	0	10	70
32	64	9	9	9	9
33	9	64	9	9	9
34	9	9	64	9	9
35	9	9	9	64	9
36	9	9	9	9	64
37	60	0	20	20	0
38	0	60	20	20	0
39	20	0	60	0	20
40	20	0	20	60	0
41	20	0	0	20	60
42	55	11	11	11	11
43	11	55	11	11	11
44	11	11	55	11	11
45	11	11	11	55	11
46	11	11	11	11	55
47	50	0	25	25	0
48	0	50	25	25	0

(conclusion)

49	25	0	50	25	0
50	25	0	0	50	25
51	25	0	25	0	50
52	45	0	28	28	0
53	28	45	0	28	0
54	28	0	45	28	0
55	0	0	28	45	28
56	28	0	28	0	45
57	37	21	21	21	0
58	21	37	21	21	0
59	21	0	37	21	21
60	21	0	21	37	21
61	0	21	21	21	37
62	33	33	33	0	0
63	33	0	33	33	0
64	33	0	0	33	33
65	33	33	0	33	0
66	0	0	33	33	33
67	33	0	33	0	33
68	100	0	0	0	0
69	0	100	0	0	0
70	0	0	100	0	0
71	0	0	0	100	0
72	0	0	0	0	100

APPENDIX B

Figure 20 – Terrain slope of sub catchments 1, 2 and 3, respectively.

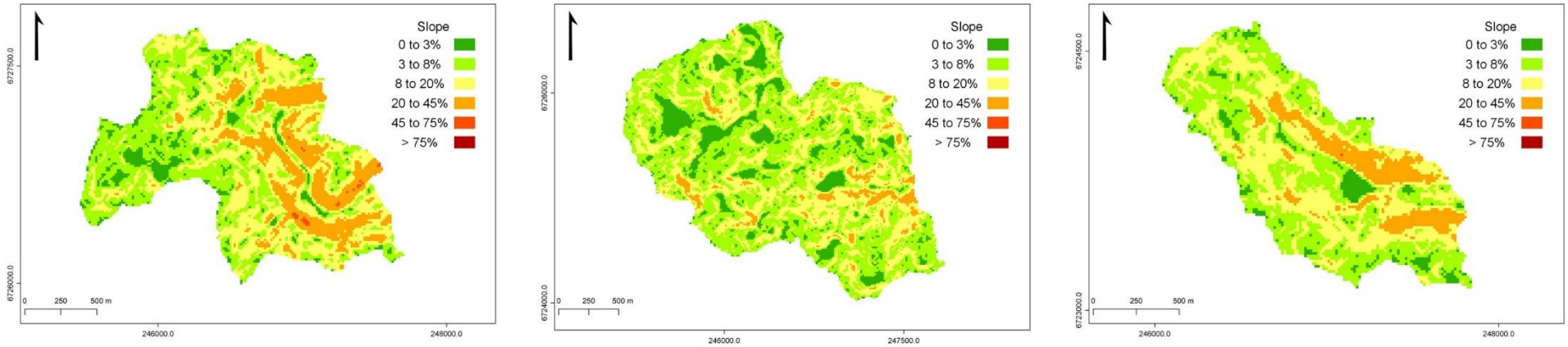

Source: Author.

Figure 21 – Plan and profile curvatures of sub catchments 1, 2 and 3, respectively.

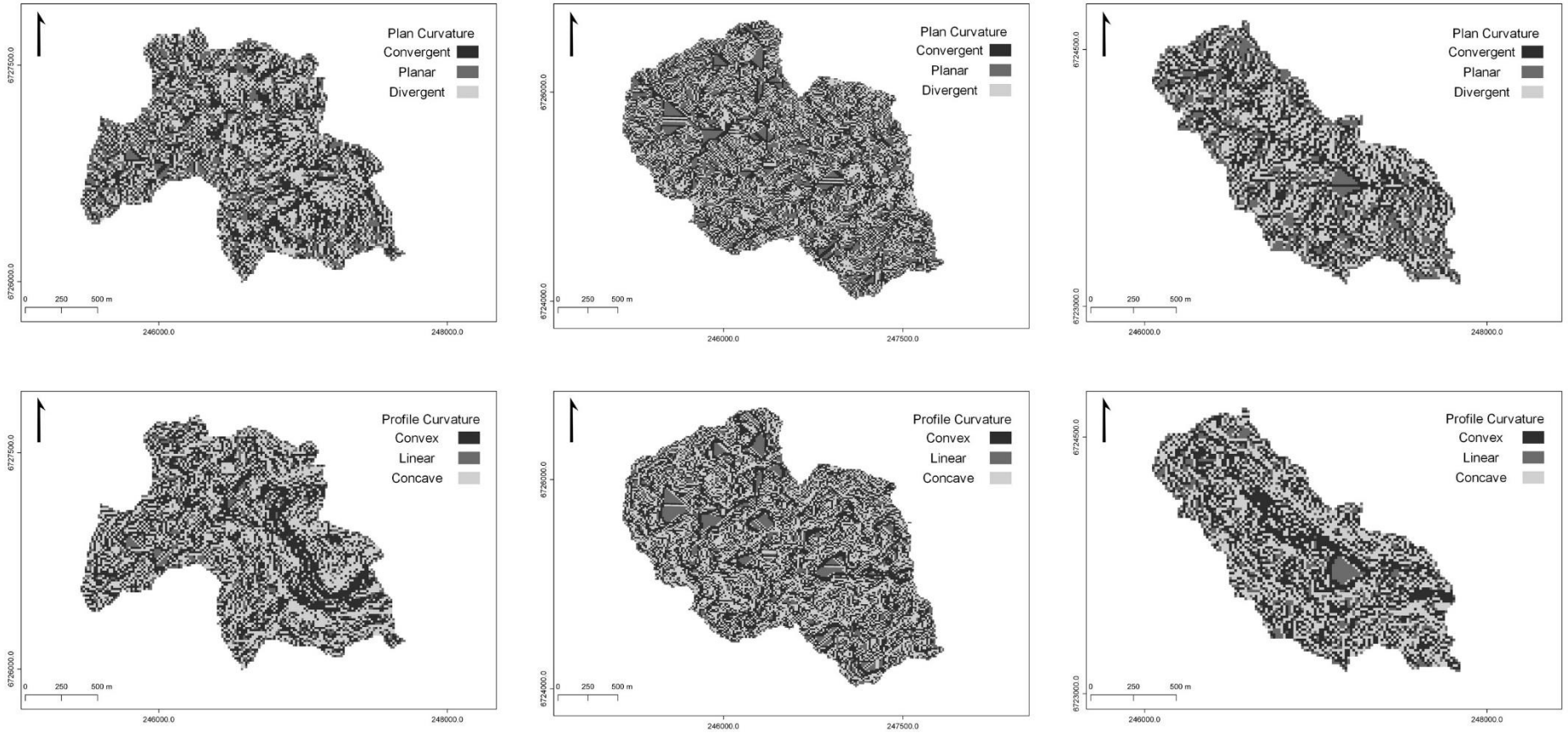

Source: Author.

Figure 22 – Topographic Wetness Index of sub catchments 1, 2 and 3, respectively.

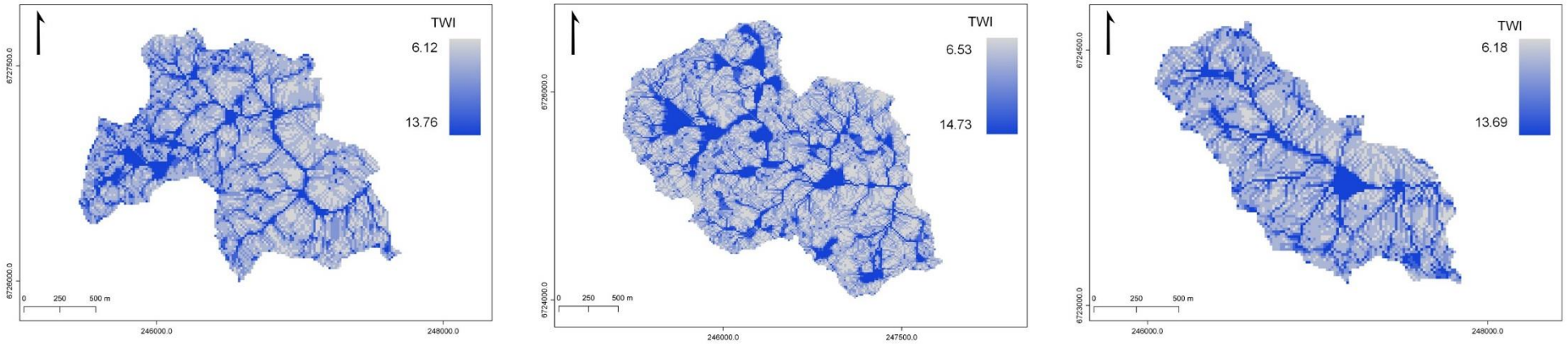

Source: Author.

Figure 23 – Stream Power Index (SPI) of sub catchments 1, 2 and 3, respectively.

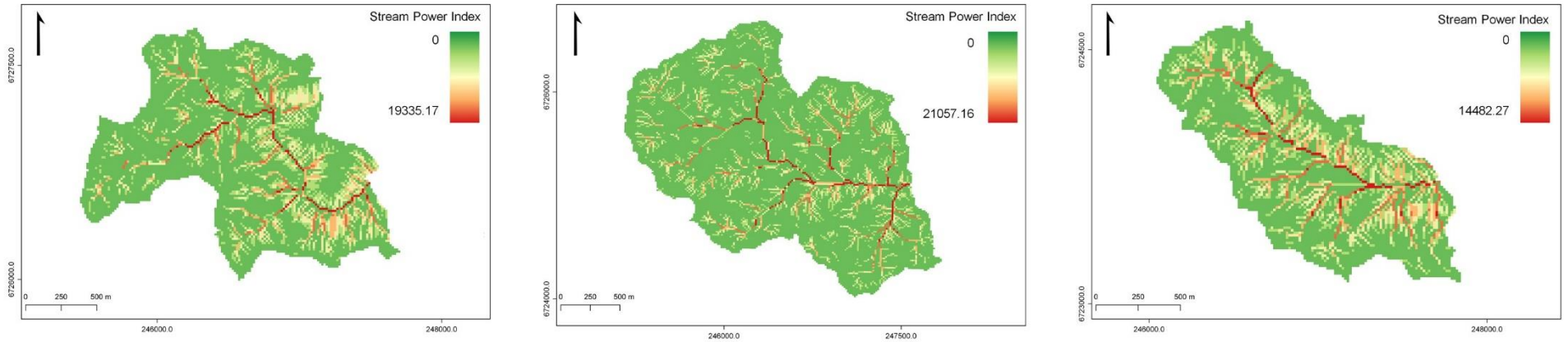

Source: Author.

Figure 24 – LS Factor of sub catchments 1, 2 and 3, respectively.

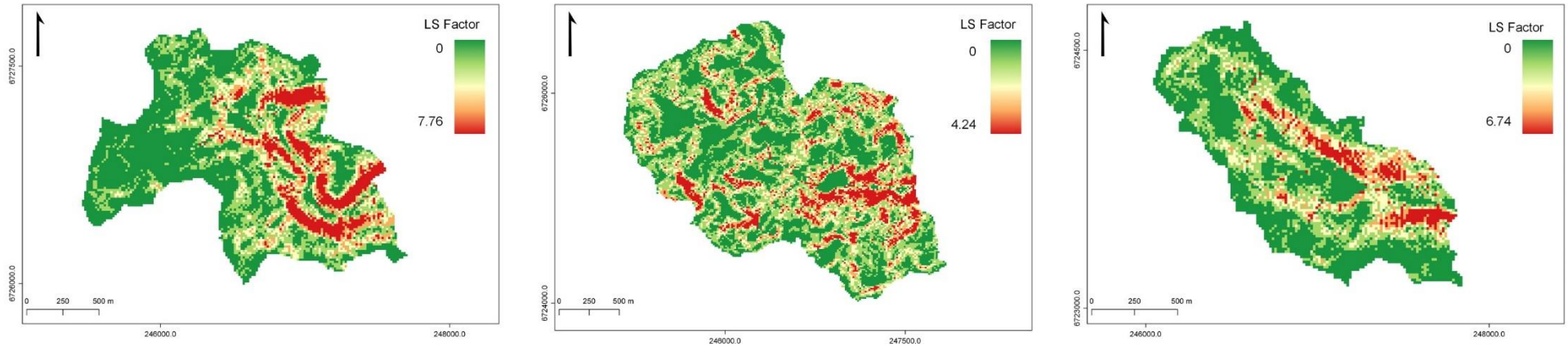

Source: Author.

APPENDIX C

Figure 25 – Maps for sediment yield and surface runoff modelling results for event 1. Sub catchments 1, 2 and 3, respectively.

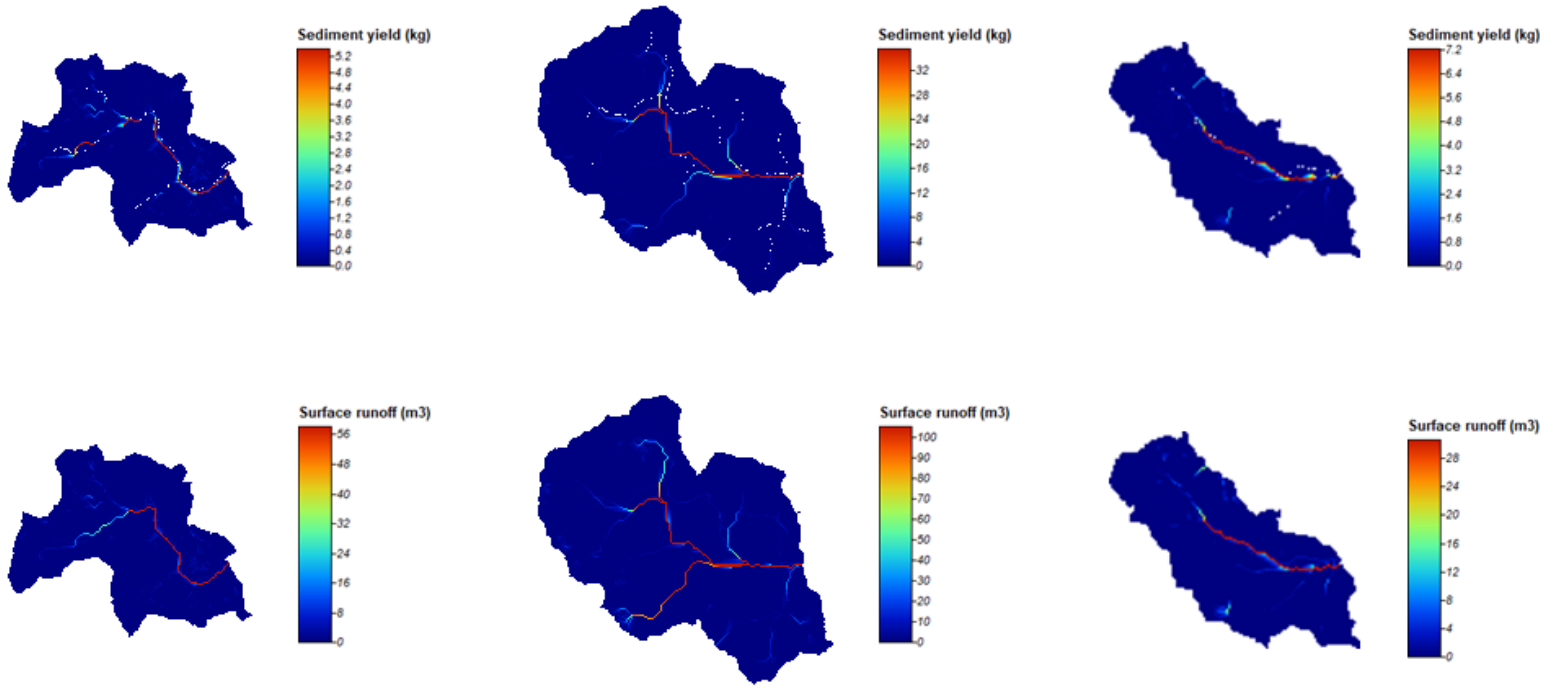

Source: Author.

Figure 26 – Maps for sediment yield and surface runoff modelling results for event 2. Sub catchments 1, 2 and 3, respectively.

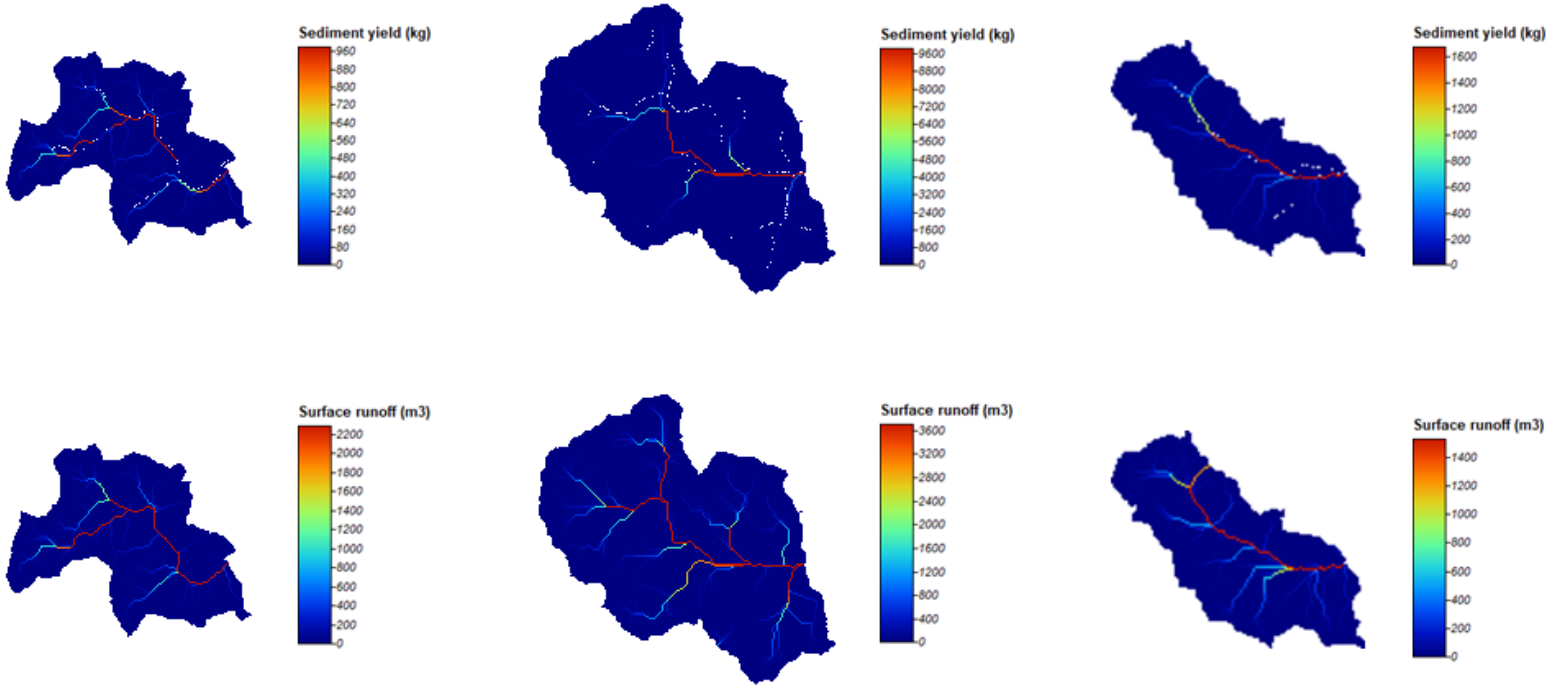

Source: Author.

Figure 27 – Maps for sediment yield and surface runoff modelling results for event 3. Sub catchments 1, 2 and 3, respectively.

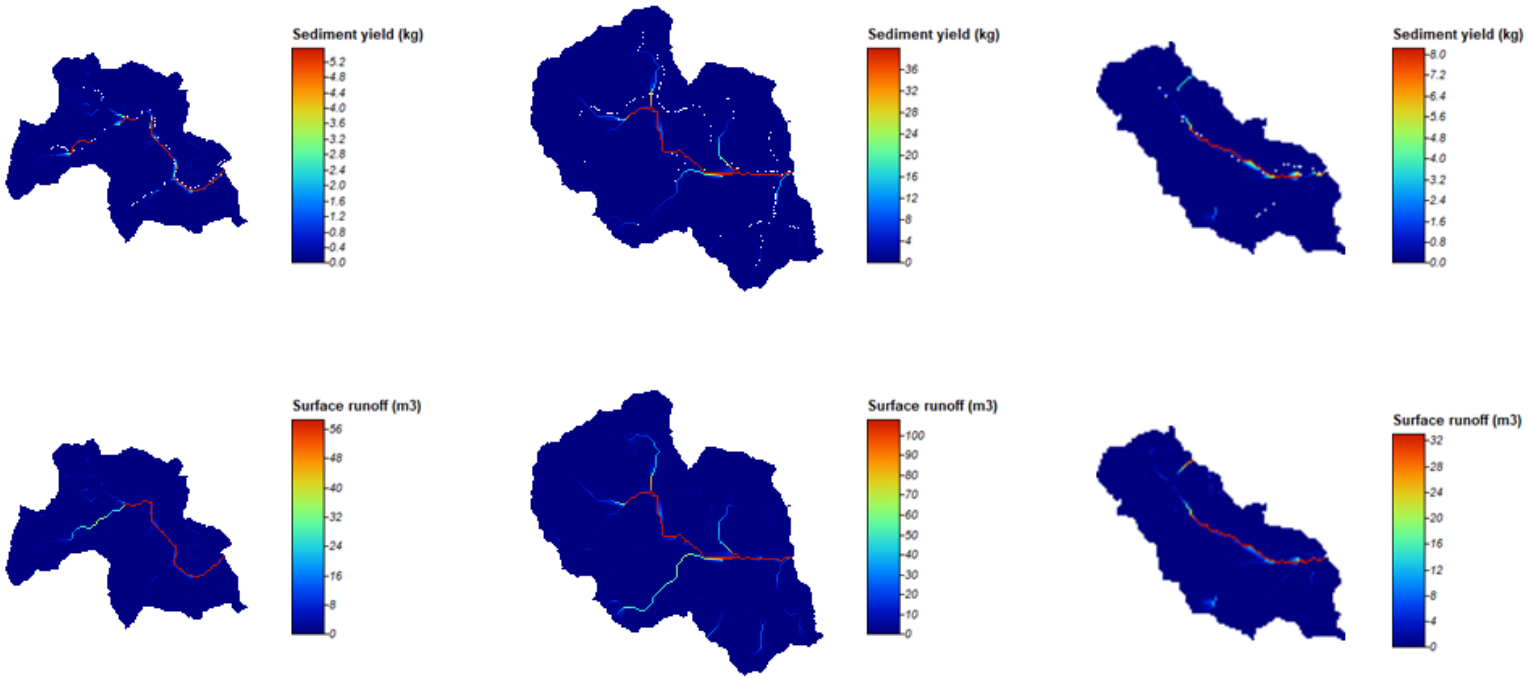

Source: Author.

Figure 28 – Maps for sediment yield and surface runoff modelling results for event 4. Sub catchments 1, 2 and 3, respectively.

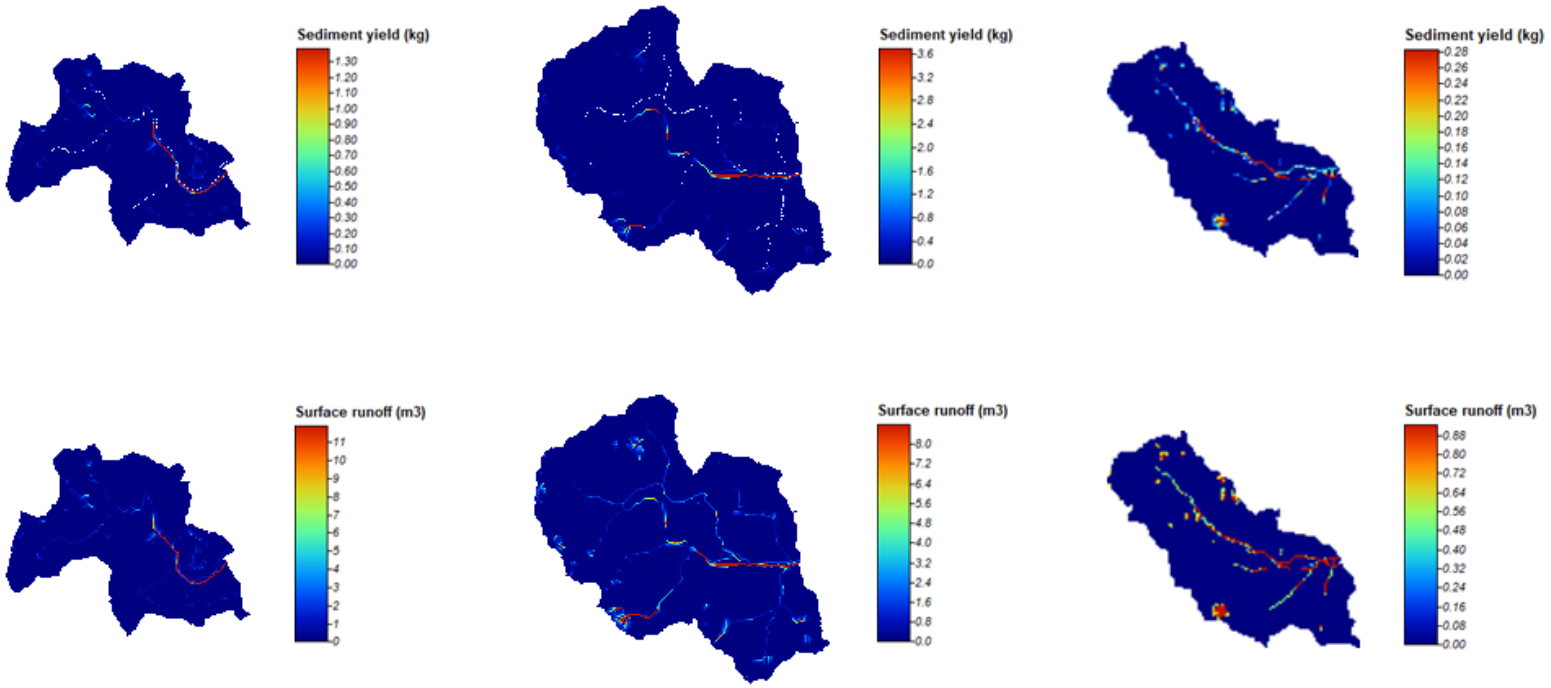

Source: Author.

APPENDIX D

Figure 29 – Model calibration and validation results for artificial mixtures from fingerprinting GMex. A = model for S1, B = model for S2, C = model for S3.

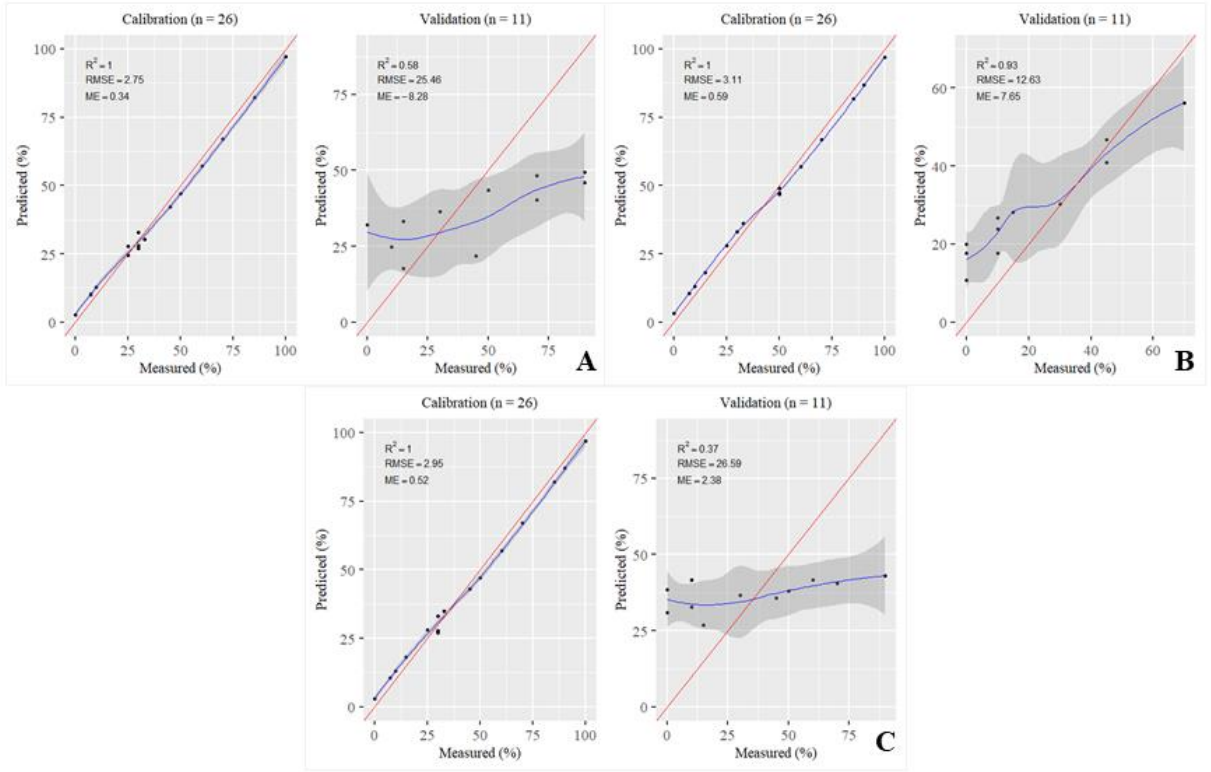

Source: Author.

APPENDIX E

Figure 30 – Model calibration and validation results for artificial mixtures from fingerprinting sub catchment 1. A = model for topsoil, B = model for stream channel, C = model for unpaved roads, D = model for forest.

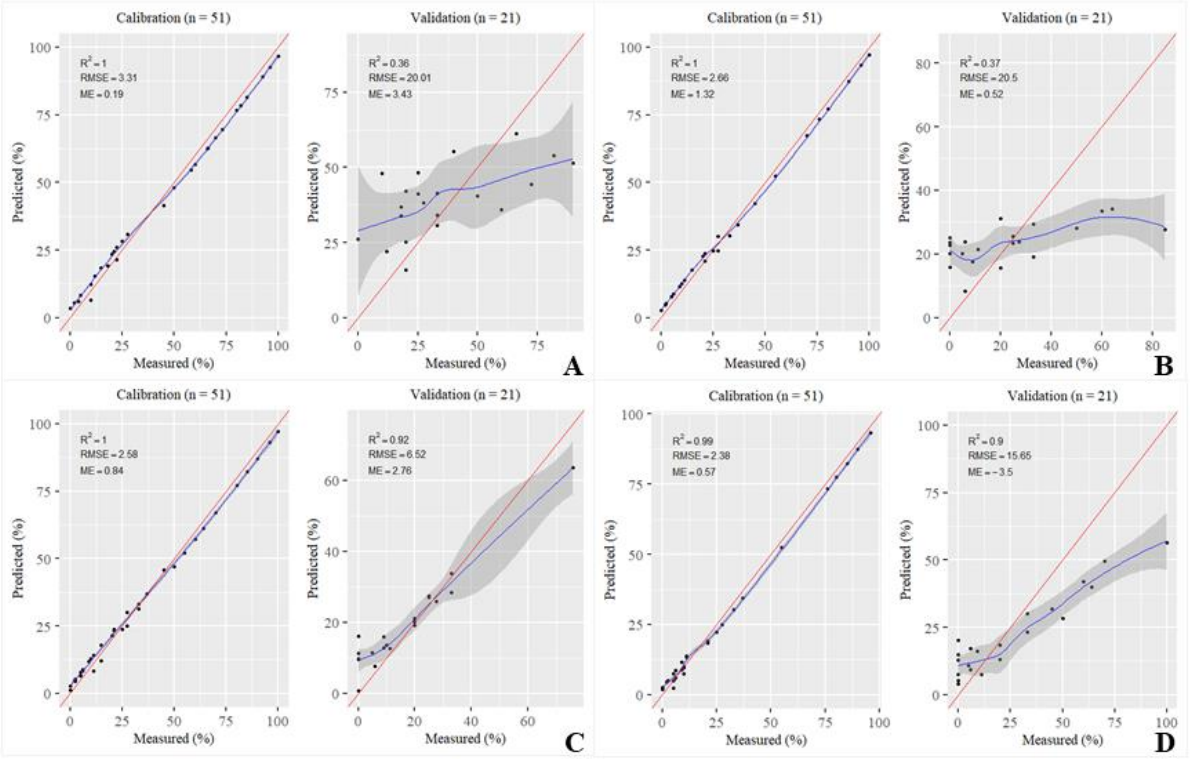

Source: Author.

APPENDIX F

Figure 31 – Model calibration and validation results for artificial mixtures from fingerprinting sub catchment 2. A = model for topsoil, B = model for stream channel, C = model for unpaved roads, D = model for forest.

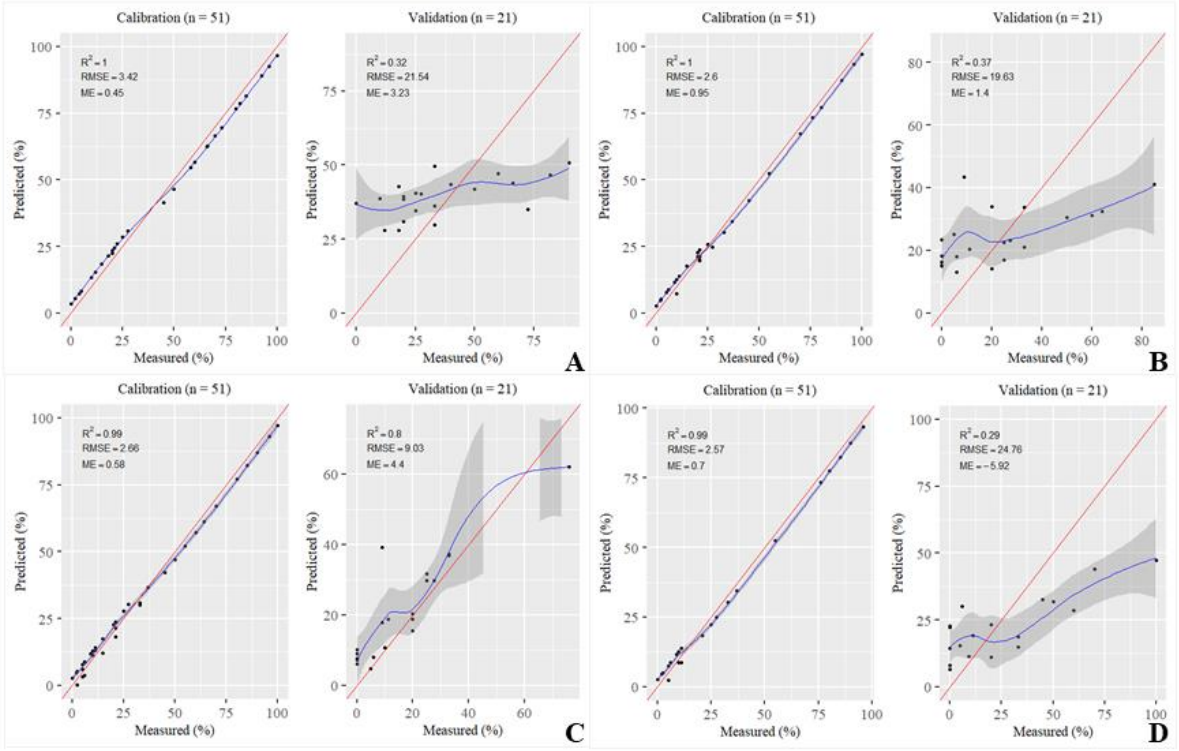

Source: Author.

APPENDIX G

Figure 32 – Model calibration and validation results for artificial mixtures from fingerprinting sub catchment 3. A = model for topsoil, B = model for stream channel, C = model for unpaved roads, D = model for forest.

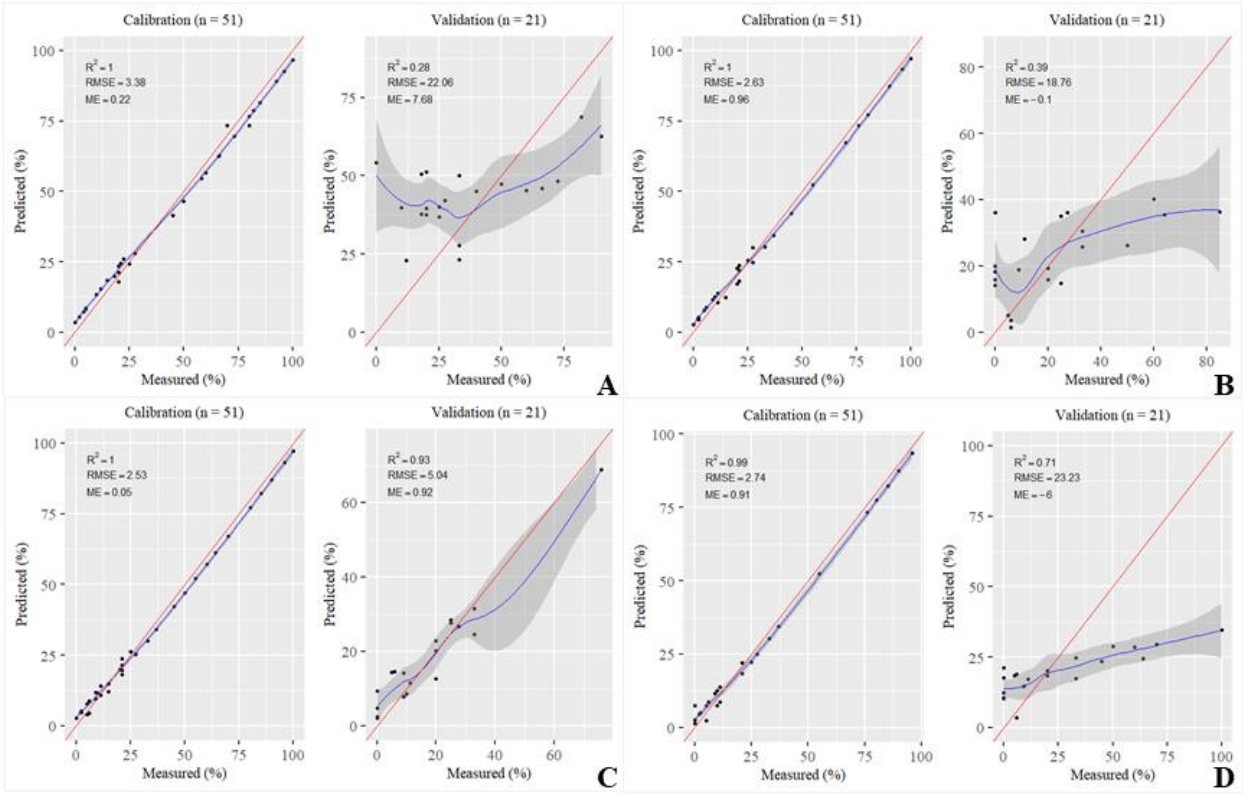

Source: Author.

APPENDIX H

Figure 33 – Boxplots for sediment source contribution in Fingerprinting 1 and Fingerprinting 2.

Source: Author.